RSC Medicinal Chemistry

ROYAL SOCIETY OF CHEMISTRY

RESEARCH ARTICLE

View Article Online
View Journal | View Issue

Cite this: *RSC Med. Chem.*, 2025, **16**, 5661

Development of novel alpha 2B adrenergic receptor ligands by using a palladium catalyzed Buchwald Hartwig amination with a brominated benzodiazepine

Maya R. T. Fernando, Alexander B. Vincent, Shaun G. Harrington, Mubaraq A. Toriola, Kayode M. Medubi, Michelle J. Meyer, Daniel A. Webb and Leggy A. Arnold *

Some benzodiazepines with excellent affinities to the gamma aminobutyric receptors have been reported to attenuate intracellular calcium by interacting with alpha adrenergic receptors (ARα). To identify novel benzodiazepines that selectively bind adrenergic receptors, we coupled amines to a brominated benzodiazepine starting material, and generated a library of compounds that yielded compounds with good affinity for the ARα_2 subtypes. These compounds were synthesized using a Buchwald Hartwig amination reaction employing XPhos as the most successful ligand among more than twenty ligands that were tested for this purpose and were part of the Catalexis screen platform from Millipore Sigma. The most promising compound has a K_i of 511 nM for the α_{2B} subtype with a 7.7-fold selectivity over the α_{2A} and 2.2-fold selectivity over the α_{2C} adrenergic receptor. Functional cell-based assays identified this compound as an ARα_{2B} antagonist. All synthesized compounds exhibited a good safety profile *in vivo* and did not influence sensorimotor coordination and behavior in mice. Overall, these findings confirm the adaptability of the benzodiazepine scaffold in medicinal chemistry enabling future work to fine-tune these compounds to develop a more potent and selective ARα_{2B} ligand.

Received 12th July 2025,
Accepted 10th September 2025

DOI: 10.1039/d5md00611b

rsc.li/medchem

1. Introduction

Diazepines are compounds containing a seven-membered heterocycle with two nitrogen atoms and are versatile scaffolds commonly employed in small molecule therapeutics. They are referred to as privileged scaffolds, as their structural pattern appears more frequently than others among successful receptor ligands.[1] Some of the most well-known diazepines are benzodiazepines that target, among other proteins, the $GABA_A$ receptors.[2] However, the structure of diazepines allows for multiple functionalities to be introduced and modulated to develop selective and potent compounds for various other targets. For example, benzodiazepines have been used to develop inhibitors of the hepatitis C virus polymerase,[3] agonists of melanocortin receptors to potentially treat obesity,[4] and antagonists of the p53–mdm2 interaction to inhibit tumor growth.[5] The structures of these compounds are shown in Fig. 1.

Department of Chemistry and Biochemistry and the Milwaukee Institute for Drug Discovery, University of Wisconsin-Milwaukee, Milwaukee, Wisconsin 53211, USA. E-mail: arnold2@uwm.edu

In this work, we describe the development of benzodiazepine-based compounds that target the alpha-2B adrenergic receptor (ARα_{2B}). There are three subtypes of the alpha 2 adrenergic receptor, ARα_{2A}, ARα_{2B}, and ARα_{2C}. These G-protein coupled receptors are located in the central and peripheral nervous systems, mediating the effects of norepinephrine.[6] They work through the function of $G_{i/o}$ proteins causing an inhibition of adenylyl cyclase and formation of cyclic AMP (cAMP).[7] The ARα_{2A} and ARα_{2C} subtypes are found mainly in the central nervous system, where the decrease of cAMP leads to a decreased amount of intracellular calcium causing the inhibition of norepinephrine release, providing an important negative feedback loop.[7] Activation of these receptors has been reported to cause sedative and analgesic effects, as well as block withdrawal symptoms in chronic opioid users.[8–10] The ARα_{2B} subtype can be found on vascular smooth muscle where activation leads to vasoconstriction and has been predicted to be required for the development of salt-induced hypertension.[11,12] The antinociceptive effect of N_2O has also been reported to require ARα_{2B} expressed in the peripheral nervous system. One study showed that mice deficient in this

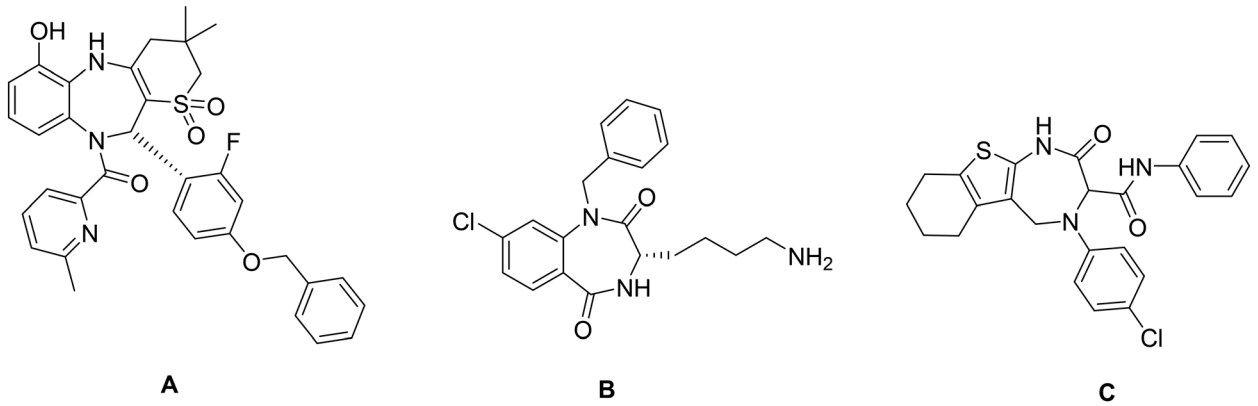

Fig. 1 Structures of diazepine compounds that target A hepatitis C polymerase, B the melanocortin receptors, and C the p53–mdm2 interaction.

subtype show little to no antinociceptive effects, while mice deficient in $AR\alpha_{2A}$ or $AR\alpha_{2C}$, respond normally.[13]

Some commonly prescribed $AR\alpha_2$ agonists include methyldopa for the treatment of hypertension, clonidine for hypertension and ADHD in children, and dexmedetomidine for sedation.[14–17] $AR\alpha_2$ antagonists are not widely used, however there are some studies that show these may be useful in reversing the effects of alpha-2 agonists, as well as having potential applications in aiding in motor recovery after brain damage,[18,19] depression[20] and Alzheimer's disease.[21]

Due to the structural similarities of alpha-2 receptor isoforms, subtype selective ligands are limited.[22] The activation or inhibition of each individual subtype has distinct biological responses, therefore developing subtype specific ligands is of high interest to increase effectiveness and reduce side effects. Although there have been a few studies that propose diazepine structures may act on adrenergic receptors, there are currently no known diazepines that specifically target the alpha-2 receptor.[23] This work gives rise to further therapeutic uses of diazepine compounds supporting our understanding of the biological importance of these receptors, specifically the $AR\alpha_{2B}$.

2. Results and discussion

2.1 Design and synthesis of novel alpha 2 receptor ligands

To develop new amine containing benzodiazepines, a previously synthesized benzodiazepine (compound **1**) was used as starting material for a Buchwald–Hartwig amination.[24] The reaction couples amines with aryl halides and we adapted a protocol from previous reports.[25,26] Our reaction was substrate specific and catalyzed by specific phosphine ligands with unique electronic and steric properties. To determine the best ligand for this specific reaction, we started investigating the coupling of compound **1** with aniline. Ligands that are part of Millipore Sigma's Catalexis program[27] were screened in the presence of $Pd_2(dba)_3$ and potassium *t*-butoxide (KO*t*Bu) (Table 1), in toluene at 90 °C for 16 hours.[28] The crude reaction mixtures were analyzed by liquid chromatography to determine percent conversions to the desired product. The reactions that produced less than 100% conversion to the desired product still had unreacted starting material.

The most successful ligands were DavePhos (L1), XPhos (L2), JohnPhos (L3), 2-(di-*tert*-butylphosphino)-1-phenylindole (L4), and APhos (L5) (Fig. 2).

Buchwald-type ligands L1, L2 and L3 gave excellent conversions. These dialkyl substituted biphenyl phosphine ligands have proven to be very stable and are frequently employed in C–N bond formations.[28] The phosphorus being in the *ortho* position (L2, L3) rather than the *meta* position (L1), gave better results, with L2 showing 100% conversion (Table 1, entry 13). L4 and L5 are not common Buchwald-type ligands but share the di-*t*-butyl substitution of the phosphine with L3. Further investigation into the reaction using L2 demonstrated that complete conversion to the product was observed within 2 h. Therefore, XPhos (L2) was selected as the ligand for subsequent reactions. The chloro analog of **1** did not react under these conditions. The final optimized reaction conditions include 1.0 eq. of the aryl bromide, 1.2 eq. of aniline, 5 mol% $Pd_2(dba)_3$, 10 mol% Xphos, 1.4 eq. of KO*t*Bu in 2 mL of toluene under N_2 at 90 °C. Under these conditions, product **2** was obtained in 87% isolated yield.

With the reaction conditions optimized, the scope of possible amines for this reaction were investigated next (Table 2).

The formation of product was observed within 2–24 hours, with yields ranging between 23–89%. The lower yielding reactions were mostly due to incomplete conversion of the starting material. Overall, *para* substituted anilines were coupled successfully, with tolerability for a wide range of substituents with different electronic properties. The only *para* substituted aniline that gave difficulties was 4-aminophenol, resulting in compound **10**. The initial attempt to synthesize compound **10** using the optimized conditions did not result in any product. This is most likely because deprotonation of the hydroxyl hydrogen instead of the amine hydrogen hindered the amination reaction from occurring. Increasing the equivalents of amine and base

Table 1 Screening of different phosphorous palladium ligands[a]

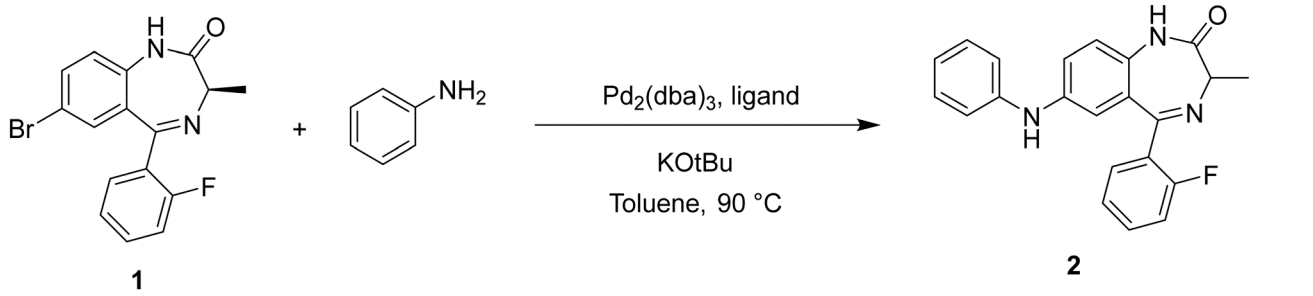

Entry	Ligand	Conversion[b] (%)
1	Trioctylphosphine	0
2	Methyldiphenylphosphine	0
3	Tris(diethylamino)phosphine	0
4	Tri(*o*-tolyl)phosphine	0
5	Tri(*p*-tolyl)phosphine	0
6	Tris(pentafluorophenyl)phosphine	0
7	Tripropylphosphine	0
8	Diphenyl-2-pyridylphosphine	0
9	Tris(dimethylamino)phosphine	0
10	Tris(2,4,6,-trimethylphenyl)phosphine	0
11	Tris(4-methoxyphenyl)phosphine	0
12	DavePhos	67
13	Xphos	100
14	JohnPhos	89
15	(3a*R*,8a*R*)-(−)-(2,2-Dimethyl-4,4,8,8-tetraphenyl-tetrahydro-[1,3]dioxolo[4,5-e][1,3,2]dioxaphosphepin-6-yl)dimethylamine	0
16	2-(Di-*tert*-butylphosphino)-1-phenylindole	100
17	APhos	81
18	*t*BuBrettPhos	0
19	Bis[2-(trimethylsilyl)ethyl] *N*,*N*-diisopropylphosphoramidite	0
20	Exo-4-anisole Kwon [2.2.1] bicyclic phosphine	0
21	HandaPhos	1
22	Bis(3,5-bis(trifluoromethyl)phenyl) (2′,6′-bis(isopropoxy)-3,6-dimethoxybiphenyl-2-yl)phosphine	0
23	Triphenylphosphite	0

[a] Reaction conditions: 1.0 mmol of aryl halide, 1.2 mmol of aniline, 5 mol% $Pd_2(dba)_3$, 10 mol% ligand, 1.4 mmol KO*t*Bu and 2 mL of toluene at 90 °C. [b] Conversion was determined by LCMS.

resulted in formation of the product in 23% yield. *Meta* and *ortho* substituted anilines, resulting in compounds **13–19**, coupled successfully with only a slight decrease in yields compared to the *para* substituted products. Regardless of the position of substituent, some substituted anilines that contained more polar groups, such as the methyl sulfone substituent **8**, caused the reaction solutions to become very heterogeneous preventing these solutions from stirring properly and leading to low conversions. Using a mixture of THF and toluene as solvent allowed all reactants to stay in solution overcoming this issue. However, the use of toluene was advantageous for product **22**, which precipitated out of the solution after full conversion of the starting material. The solid was collected by vacuum filtration, dried in a vacuum oven, and analyzed to show good purity (94%) and 71% yield. To investigate the synthetic potential of this

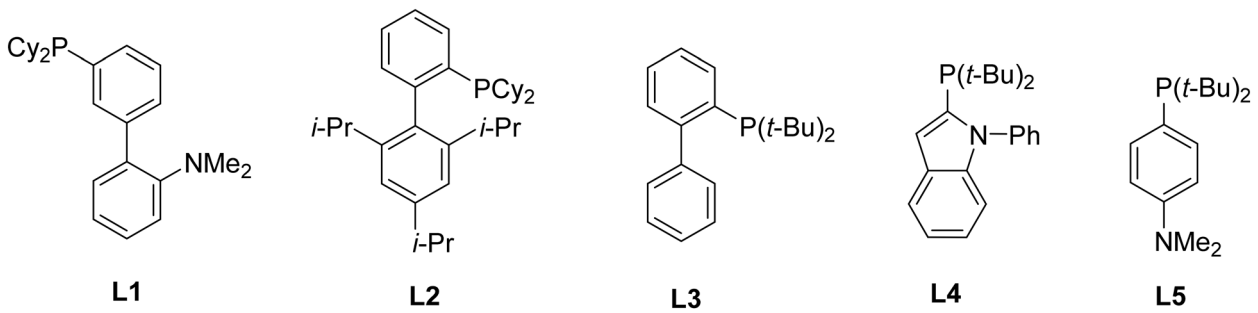

Fig. 2 Successful ligands used in the amination of **1** and aniline.

Table 2 Application of various amines[a]

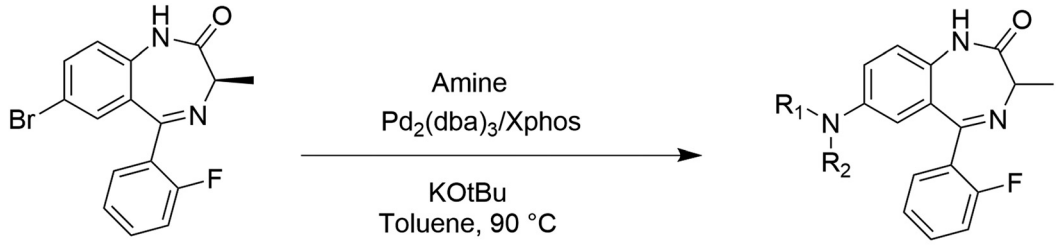

Compound	Amine	Yield[b] (%)	% e.e.
2	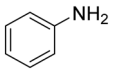	87	1.4
3	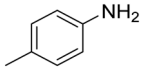	78	0.8
4	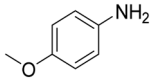	81	1.2
5	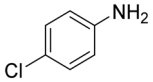	75	1.8
6	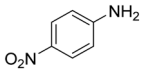	84	2.0
7	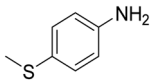	58	0.2
8[c]	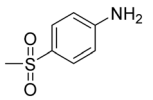	80	44.8
9[d]	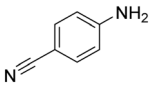	89	0.6
10[e]	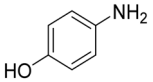	23	76.4
11	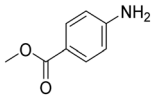	65	1.4
12	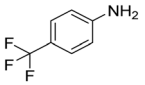	64	0.4
13[d]	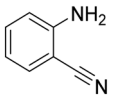	50	0.4
14	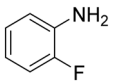	45	4.4
15	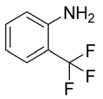	48	0.8
16	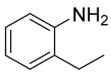	36	9.8
17	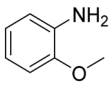	79	0.2

Table 2 *(continued)*

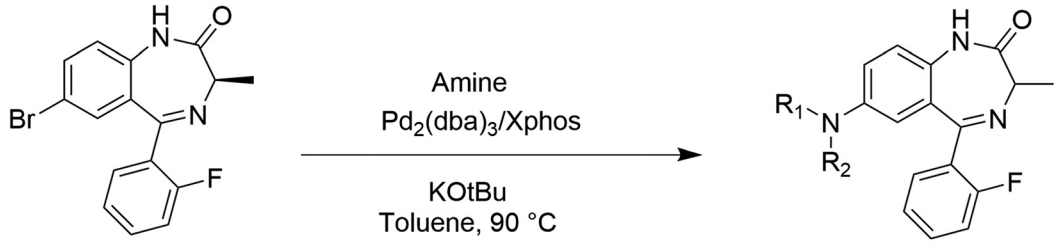

1 **2-27**

Compound	Amine	Yield[b] (%)	% e.e.
18	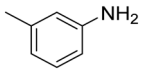	68	2.0
19[d]	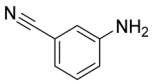	57	0.4
20	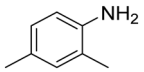	83	1.0
21	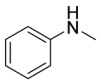	44	0.4
22[f]		71	0.4
23[f]		58	0.2
24[f]	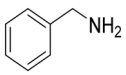	64	1.0
25		71	4.4
26[g]	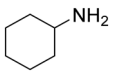	81	2.2
27[h]		76	1.8

[a] Reaction conditions: 0.5 mmol of aryl halide, 1.2 eq. of aniline, 5 mol% $Pd_2(dba)_3$, 10 mol% ligand, 12.2.4 eq. KO*t*Bu and 2 mL of toluene at 90 °C. [b] Isolated yields reported. [c] 5 mL of a 30% THF in toluene solution used as solvent. [d] 5 mL of a 20% THF in toluene solution used as solvent. [e] 3 eq. of aniline and 3.5 eq. of KO*t*Bu used. [f] 1.4 eq. of amine and 1.5 eq. of KO*t*Bu used. [g] 40% ligand, 2.3 eq. of amine, 1.3 eq. of KO*t*Bu and 5 mL of toluene used. [h] 30% ligand, 2.5 eq. of amine, 1.7 eq. of KO*t*Bu and 5 mL of toluene used.

phenomenon, compound **2** was generated on a 10 mmol scale using toluene. After 4 hours of stirring, all starting material was consumed and like **22**, compound **2** precipitated out of solution after cooling down to room temperature. Filtration afforded compound **2** in 84% yield. This demonstrates that these reaction conditions are suitable for larger scale synthesis with minimal purification with the use of toluene. The *N*-substituted aniline **21** also formed the corresponding amination product increasing the range of this reaction to secondary amines. In addition, the reaction conditions were successful for coupling non-aromatic heterocyclic amines like morpholine and piperidine, as well as a benzylamine, resulting in compounds **22**, **23** and **24**. Lastly, small primary aliphatic amines including *t*-butylamine, cyclohexylamine and dimethylamine formed compounds **25**, **26** and **27**. Most products were purified by filtration through a pad of celite to remove any solids followed by several washes with acetone. The solvents were evaporated, and the crude product was purified by column chromatography (silica) employing a gradient of acetone in hexanes. All products were obtained in high purity. Most products were obtained as racemates starting from optical pure **1**, due to the use of strong base *t*-BuOK. We reported the formation of the racemate **1**, when ring cyclization was performed in the present of strong bases such as NaOH.[24] Interestingly, we obtained compound **8** with an ee of 44.8% and **10** with 76.4% ee. We are currently in the process to develop a stereospecific synthetic method.

Table 3 Physiochemical properties

Compound	Aqueous solubility[a] (μM)	Cytotoxicity[b] LD_{50} (μM)	$AR\alpha_{2A}$ binding[c] (% inhibition at 10 μM) (K_i (nM))	$AR\alpha_{2B}$ binding[c] (% inhibition at 10 μM) (K_i (nM))	$AR\alpha_{2C}$ binding[c] (% inhibition at 10 μM) (K_i (nM))
1	35.7 ± 1.70	>300	11	−6	1
2	2.17 ± 0.47	100 ± 19	66 (3933)	90 (511)	84 (1127)
3	4.33 ± 0.31	62 ± 15	66 (2282)	61 (4638)	59 (2161)
4	<1	87 ± 32	70 (2072)	41	55 (2082)
5	6.83 ± 0.52	87 ± 36	78 (2085)	81 (1412)	88 (1640)
6	<1	61 ± 10	52 (2620)	36	41
7	3.69 ± 1.16	63 ± 12	65 (3297)	41	69 (2407)
8	34.0 ± 4.40	>150	10	−5	7
9	3.57 ± 0.96	83 ± 29	49	23	47
10	197.9 ± 4.04	135 ± 26	36	52 (4183)	29
11	<1	88 ± 17	77 (2253)	44	65 (1545)
12	1.44 ± 0.28	>150	60 (2586)	38	34
13	6.98 ± 0.78	>150	38	29	34
14	26.0 ± 2.10	90 ± 27	63 (2244)	82 (1276)	58 (2135)
15	8.09 ± 0.65	69 ± 42	24	32	16
16	<1	>300	4	−2	−11
17	3.90 ± 0.45	148 ± 12	74 (2052)	91 (607)	62 (738)
18	3.52 ± 2.04	109 ± 12	65 (2081)	87 (1671)	69 (1178)
19	1.35 ± 0.14	165 ± 27	38	57 (3249)	8
20	1.38 ± 1.07	88 ± 22	31	33	5
21	<1	158 ± 27	48	47	15
22	157.3 ± 5.50	>300	−4	27	30
23	100.5 ± 4.00	>300	9	61	31
24	1.35 ± 0.64	>150	15	46	47
25	393.6 ± 10.40	>300	6	40	35
26	21.4 ± 0.80	>300	61	64	80
27	186.5 ± 2.70	>300	41	45	28

[a] Shake flask, pH 7.4. [b] Cytotoxicity was determined using HEK293 cells using CellTiter-Glo. [c] Competition assay of $AR\alpha_2$ ligand ^{3}H-Rauwolscinein using MDCK or HEK293 cell that overexpress specific $AR\alpha_2$.

2.2 Preclinical characterization *in vitro*

The physiochemical properties of all products are summarized in Table 3. The aqueous solubility was measured using a shake flask method. Cytotoxicity was determined using embryonic kidney cells. In collaboration with the Psychoactive Drug Screening Program (PDSP),[29] compounds were screened against common central nervous system receptors to determine possible target receptors for these compounds. Among those, most compounds showed binding to the alpha-2 adrenergic receptors.

The compounds showed solubilities ranging from 1 μM to 394 μM. Overall, the substitution of the bromine by anilines decreased the aqueous solubility of the resulting benzodiazepines. The aryl substituents moderately influenced aqueous solubility. Compounds that contain substituents that can participate in hydrogen bonding like methylsulfone (compound **8**) or fluorine (compound **14**) did have slightly better aqueous solubilities with 34 μM and 27 μM, respectively. Compound **10** with a hydroxy substituent showed the highest solubility of all compounds containing aryl substituents, with 198 μM. The cyclic aliphatic amine containing compounds **22** and **23** exhibited solubilities above 100 μM. Among the benzodiazepines with aliphatic amines, compound **25** showed the highest solubility with 394 μM. Thus, benzodiazepines with arylamines were less soluble than those with alkylamine moieties. Cellular toxicity was determined by incubating embryonic kidney cells (HEK-293) with different compound concentrations for 18 h followed by quantification of cellular ATP using CellTiter-Glo (Table 3). The arylamine containing compounds **2–20** showed LD_{50} values ranging from 65 μM to higher than 300 μM. Overall, the alkylamine containing benzodiazepines were less toxic than arylamine benzodiazepines with LD_{50} values greater than 150 μM.

Receptor binding was determined using a competition assay with ^{3}H-Rauwolscinein employing membranes from cells overexpressing the three different isoforms ($AR\alpha_{2A}$, $AR\alpha_{2B}$, and $AR\alpha_{2C}$). All compounds were initially screened at 10 μM, and those that achieved more than 50% inhibition were subjected to a concentration response analysis (Table 3). Most compounds showed greater affinity to all three of the alpha 2 adrenergic receptor subtypes than our initial starting benzodiazepine. Some exhibited selectivity towards $AR\alpha_{2B}$. This leads us to believe that adding increased bulkiness to the benzodiazepine by substituting the bromine of compound **1** with an aryl substituted amine benefited binding to these specific receptors. The strongest binding in this series was observed for the phenylamine and the 2-methoxyphenylamine substituted compound **2** (K_i = 511 nM) and **17** (K_i = 607 nM) for the $AR\alpha_{2B}$. Compound **2** is moderately selective for α_{2B} over the α_{2A} subtype (7.7-fold) and weakly selective for α_{2B} over the α_{2C} subtype (2.2-fold). Compound **17** is only selective for α_{2B} over the α_{2A} subtype

(3.8-fold). For *para*-substituted compounds, only compounds **2**, **3**, **5** and **10** showed strong binding to $AR\alpha_{2B}$, which most likely shows that there is limited space in the receptor binding pocket occupying small substitutions. Some larger *para*-substituted compounds **6**, **7**, **11**, **12**, showed binding to $AR\alpha_{2A}$ or $AR\alpha_{2C}$, but not $AR\alpha_{2B}$, proving differences of binding sites of ARα isoforms. The *ortho* substituted compounds **13**, **15** and **16** showed weak binding to all 3 subtypes, again possibly indicating that larger substituents are unfavorable at this position. Compounds **14** (*o*-fluoro) and **17** (*o*-methoxy) showed good binding to $AR\alpha_{2B}$, potentially due to their smaller size and ability to form hydrogen bonds. Interestingly, placing a methoxy group in the *ortho* position (compound **17**) instead of the *para* position (compound **4**) greatly benefited binding. With this modification, the inhibition at 10 μM increased from 41% to 91% at the $AR\alpha_{2B}$. Both *meta* substituted compounds **18** and **19** showed good activities for the $AR\alpha_{2B}$ subtype with K_i values of 1671 and 3249 nM, respectively. Compound **19** also exhibited selectivity towards the $AR\alpha_{2B}$ with primary inhibition of less than 50% for the other two receptor subtypes. The addition of multiple aryl substituents (**20**) or using an *N*-methylated aniline (**21**) led to lower receptor affinity. Finally, of the compounds containing non-aromatic amine substituents, only **23** and **26** showed binding above 50% at 10 μM potentially demonstrating that aryl amine substituted benzodiazepines are superior ligands for the alpha-2 adrenergic receptors.

To analyze if compounds **2** and **17** activate or antagonize $AR\alpha_2$, we performed a GPCR Tango assay.[30] Briefly, $AR\alpha_2$ transfected HEK cells were treated **2**, **17** or control compound norepinephrine (Fig. 3). Activation of the receptor initiates β-arrestin recruitment linked to TEV protease, followed by cleaving the *t*TA transcription factor that in turn will activate the transcription of luciferase. The amount of luciferase was quantified by the addition of BrightGlo® (Promega).

Norepinephrine activated $AR\alpha_{2A}$, $AR\alpha_{2B}$, and $AR\alpha_{2C}$ with an EC_{50} of 98, 186, and 126 nM, respectively. Compounds **2** and **17** did not activate any of these $AR\alpha_2$ subtypes. In contrast, **2** and **17** antagonized $AR\alpha_{2A}$, $AR\alpha_{2B}$, and $AR\alpha_{2C}$ in the presence of 300 nM norepinephrine. The IC_{50} values were higher than the K_i values determined by the radioligand displacement assay (Table 3, entries 2 and 17). Usually, competition assays are more sensitive if low concentrations of activator are employed *e.g.* radiotracer competition assays. The moderate affinity of norepinephrine for the $AR\alpha_2$ subtypes requires a concentration of 300 nM for the cell-based assay that probably caused the observed IC_{50} shift for moderate binders **2** and **17**. The $AR\alpha_2$ blocker Rauwolscine antagonized $AR\alpha_{2A}$, $AR\alpha_{2B}$, and $AR\alpha_{2C}$ with an IC_{50} of 23, 22, and 10 nM, respectively. The K_i reported for Rauwolscine for $AR\alpha_{2A}$, $AR\alpha_{2B}$, and $AR\alpha_{2C}$ is 3.76, 4.59, and 0.78 nM, respectively,[31] confirming the fact that the IC_{50} determined for the cell-based assay is shifted 5 to 13-fold in comparison to the K_i determined for the radiotracer competition assay. Nevertheless, we observed full antagonism of 300 nM of norepinephrine at 30 μM of **2** or **17**.

2.3 Molecular docking

To better understand the $AR\alpha_2$ subtype selectivity of **2**, we used available receptor protein structures that included for $AR\alpha_{2A}$ (6KUX),[32] $AR\alpha_{2B}$ (6K41),[33] and $AR\alpha_{2C}$ (6KUW).[34] Protein PDB files were uploaded in MOE and prepared using

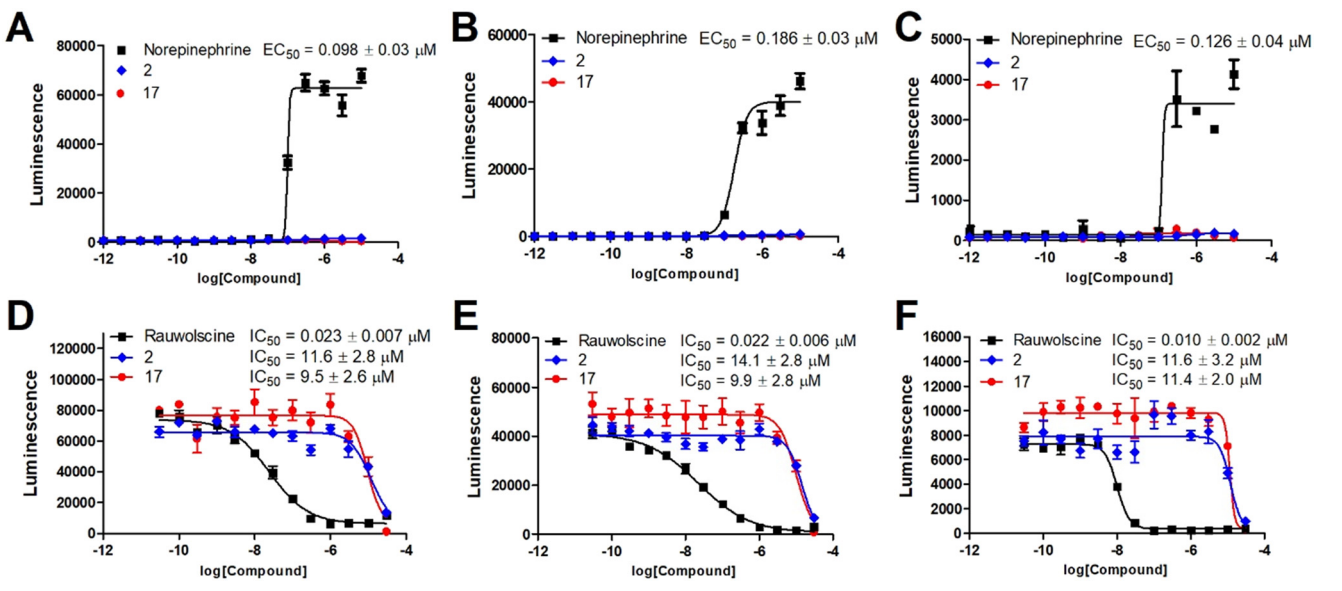

Fig. 3 Functional cell-based assay to determine the mode of action of 2 and 17. HEK293 cell transfected with $AR\alpha_{2A}$ (A), $AR\alpha_{2B}$ (B), or $AR\alpha_{2C}$ (C) were treated with norepinephrine, 2, or 17 in a concentration dependent manner for 18 h followed by the quantification of luciferase using Bright-Glo (n = 3 for each concentration); HEK293 cell transfected with $AR\alpha_{2A}$ (D), $AR\alpha_{2B}$ (E), or $AR\alpha_{2C}$ (F) were treated with 300 nM norepinephrine and Rauwolscine, 2, or 17 in a concentration dependent manner for 18 h followed by the quantification of luciferase using Bright-Glo (n = 3 for each concentration).

a structure preparation tool. Both enantiomers of **2** were docked at the ligand site using triangle matcher placement and induced fit refinement. Docking scores were calculated as London dG energies.

For $AR\alpha_{2A}$, docking scores for **2** ranged between −7.02 and −6.56 for the *R* enantiomer and −6.56 and −6.26 for the *S* enantiomer. Two H–π interactions were observed between **2** and $AR\alpha_{2A}$ (Fig. 4D). Compound **2** did not form a hydrogen bond interaction with Asp113 due to the steric interaction with Ile188 (Fig. 4A upper left corner). In addition, Phe390 significantly reduced space in the lower left corner of the $AR\alpha_{2A}$ binding side. Overall, the computational analysis confirmed that **2** had the lowest affinity for $AR\alpha_{2A}$ among the three receptors with an K_i of 3.9 μM (Table 3, entry 2). Interestingly, **6** and **12** with a nitro and trifluoro methyl group in the 4-position had better affinities for $AR\alpha_{2A}$ than **2** due possible to interactions with Ser204 (Table 3, entries 6 and 12). These compounds had poor affinities for $AR\alpha_{2B}$. Docking scores for **2** for $AR\alpha_{2B}$ ranged between −7.98 and −7.14 for the *R* enantiomer and −7.57 and −7.21 for the *S* enantiomer. The better docking scores were influenced by a hydrogen bond interaction between Asp92 and the aryl amine moiety of **2** (Fig. 4B). The amine aryl moiety of **2** fit well in the pocket created by Tyr88, Ser69, and Asn72 (Fig. 4E). In addition, the pendent 2-fluorophenyl ring occupied a pocket created by Trp384 and Tyr416. Thus, the *Y* shaped binding site of $AR\alpha_{2B}$ and hydrogen bonding with Asp92 supported a high affinity of **2** for $AR\alpha_{2B}$. For $AR\alpha_{2C}$, we calculated docking scores for **2** that ranged between −7.36 and −7.13 for the *R* enantiomer and −7.48 and −7.29 for the *S* enantiomer. The docking scores of **2** fall in between the docking scores for $AR\alpha_{2A}$ and $AR\alpha_{2B}$ aligning with order of affinities that decreases from $AR\alpha_{2B} > AR\alpha_{2C} > AR\alpha_{2A}$. We observed a hydrogen bonding between the imine of **2** and Asp131 and a H–π interaction between the aryl amine moiety and Arg192 (Fig. 4F). In comparison with $AR\alpha_{2a}$ and $AR\alpha_{2B}$ the binding pocket of $AR\alpha_{2C}$ is significant larger enabling a path forward for developing $AR\alpha_{2C}$ selective compounds by introducing additional substituents (Fig. 4C). This is supported by the fact that the introduction of a 4-methyl ester aniline (compound **11**) had a similar affinity for $AR\alpha_{2C}$ but only weak affinity for $AR\alpha_{2B}$ (Table 3, entry 11).

2.4 Preclinical characterization *in vivo*

Next, we investigated these novel compounds *in vivo* to identify any severe toxicity or CNS effects. Therefore, we used a sensorimotor assay represented by the rotarod assay and a behavioral assay represented by the open field test (OFT). $AR\alpha_2$ agonists are known to elicit sedation as demonstrated

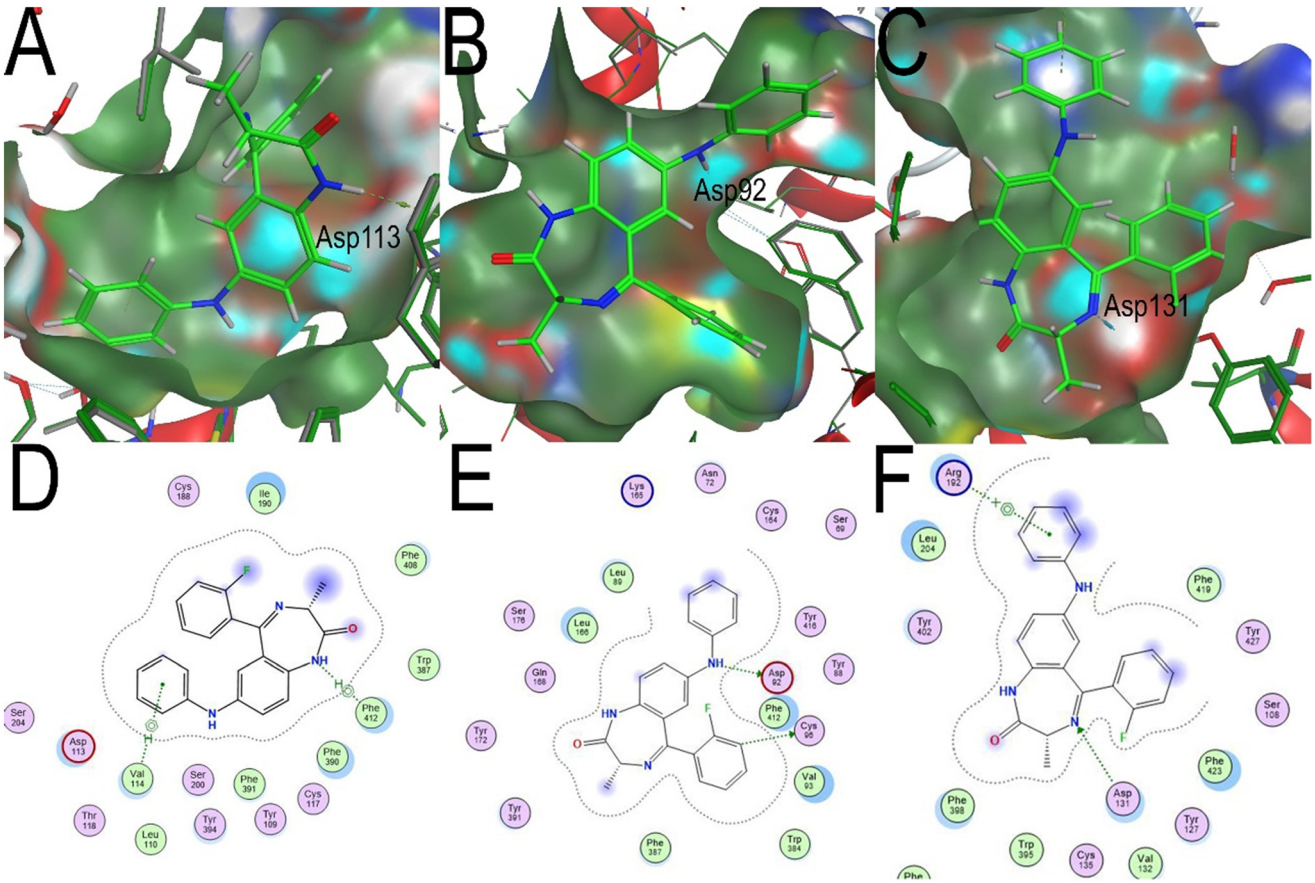

Fig. 4 Best docking poses for **2** (*R*-enantiomer): A) $AR\alpha_{2A}$, B) $AR\alpha_{2B}$, C) $AR\alpha_{2C}$, D) ligand interaction between $AR\alpha_{2A}$ and **2**, E) ligand interaction between $AR\alpha_{2b}$ and **2**, F) ligand interaction between $AR\alpha_{2C}$ and **2**.

for dexmedetomidine that reduced the ability of mice to stay on the rotating rod at i.p. doses of higher than 10 μg kg^{-1}.[35] In contrast, $AR\alpha_2$ antagonists do not usually alter the ability of mice to complete a rotarod exercise, which was demonstrated by the administration of phentolamine at 4 mg kg^{-1} (i.p.).[36] Consistent with these findings, we did not observe any sensorimotor inhibition with $AR\alpha_2$ antagonists **2** and **17** when measured after 10, 30 and 60 minutes (Fig. 5A summarizes data at 30 min whereas 10 min and 60 min data can be found in the SI). To ensure that compounds, specifically **2**, are orally available, we performed a limited pharmacokinetic study with a dose of 40 mg kg^{-1} (Fig. 5B). As early as 10 min, we found an appreciable concentration of **2** in blood and brain that exceeded the affinity of **2** for the target receptor. The concentrations of **2** increased at 30 min and declined at 60 min. The blood : brain ratios increased over time.

$AR\alpha_2$ ligands have also been studied with the OFT quantifying movements and activity.[37] It was reported that α_2 agonist dexmedetomidine administered at 30 μg kg^{-1} (s.c.) significantly reduced the activity scores whereas $AR\alpha_2$ antagonist atipamezole did not modulate locomotion at a dose of 1 mg kg^{-1}. We administered compounds **2–27** at 40 mg kg^{-1} and evaluated locomotion after 40 min. The results for **2** and **17** are depicted in Fig. 6, whereas data for all other compounds are included in the SI. For this study, we quantified total distance traveled for the duration of 3 min as well as average speed, total time freezing (no body and distance movement), total time mobile and total time immobile (including body movement like grooming).

Vehicle and compound treated mice exhibited similar behavior and the collected data showed no significant differences between the vehicle group and compound groups for the determined parameters. Thus, all newly synthesized compounds showed a good safety profile at 40 mg kg^{-1}. Compounds **2** and **17** with significant affinity towards $AR\alpha_{2A}$, $AR\alpha_{2B}$, and $AR\alpha_{2C}$ showed no sedation confirming the functional receptor binding data that these compounds are $AR\alpha_2$ antagonists rather than $AR\alpha_2$ agonists.

3. Conclusions

It can be concluded that benzodiazepines bearing an aryl amine substituent can bind $AR\alpha_2$ with nanomolar affinities resulting in receptor antagonism. Large aryl substituents reduced binding of the corresponding ligands for $AR\alpha_{2B}$ revealing a limited receptor binding pocket that resulted in subtype selectivity for unsubstituted compound **2**. *In vivo* and *in vitro* studies showed that these ligands have a good safety profile and in case of **2** are orally available. The observed subtype selectivity of these ligands is promising and represents one of the goals of future research in addition to improved receptor affinity and better aqueous solubility.

4. Experimental

Chemicals and solvents were purchased from commercial sources and used without further purification. Reaction progress was monitored by silica gel TLC (Dynamic Adsorbents Inc.) with fluorescence indicator. ^{1}H and ^{13}C-NMR spectra were obtained on Bruker 400 MHz or 500 MHz instruments with the chemical shifts in δ (ppm) reported by reference to the deuterated solvents as an internal standard DMSO-d_6: δ = 2.50 ppm (^{1}H-NMR) and δ = 39.52 ppm (^{13}C-NMR) (see SI for NMR spectra). HRMS spectral data were recorded using a LCMS QTOF spectrometers (Shimadzu). High performance liquid chromatography (Shimadzu Nexara series HPLC) coupled with a photo diode array detector (PDA, Shimidzu SPD-M30A) and a single quadrupole mass analyzer (LCMS 2020, Shimadzu, Kyoto, Japan) was used for purity

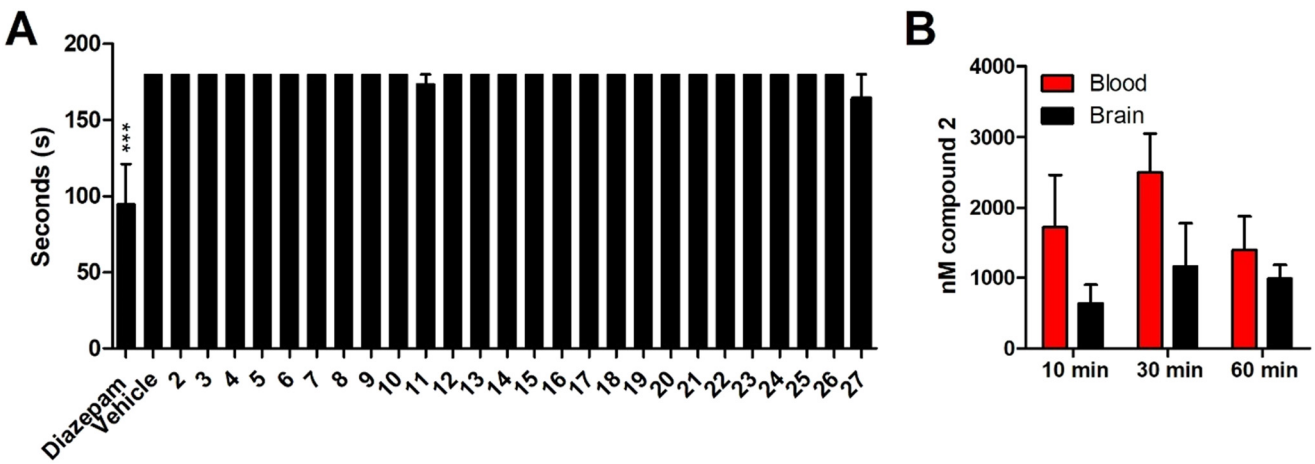

Fig. 5 A) Rotarod studies. Female Swiss Webster mice were monitored on a rotarod apparatus for 3 min at 10, 30, and 60 min after oral administration of 40 mg kg^{-1} of compound. The presented data is 30 min. The time of fall was recorded if it occurred within 3 min. Data are expressed as means ± SEM (n = 8). Significance was calculated with 2-way ANOVA in respect to vehicle. B) Pharmacokinetic study. 40 mg kg^{-1} of **2** was administrated orally to female Swiss Webster mice (n = 4) and brain and blood concentrations were determined at 10, 30, and 60 min. Data are expressed as means ± SEM (n = 4).

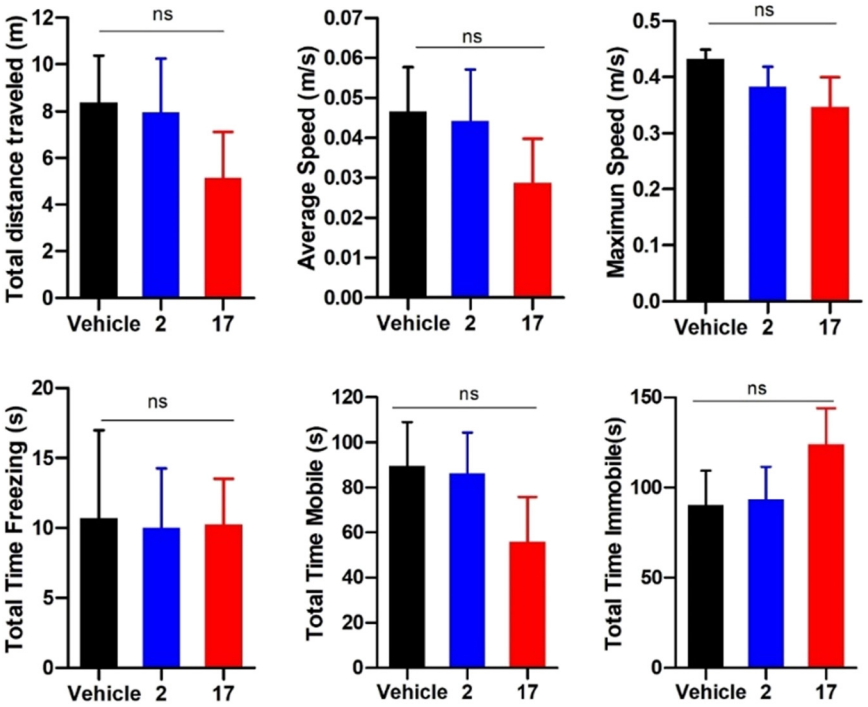

Fig. 6 Open field test. Locomotion of female Swiss Webster mice was monitored in a 40 cm^2 box arena for 3 min 40 minutes after oral administration of 40 mg kg^{-1} of compound. Data are expressed as means ± SEM (n = 6). Significance was calculated using one-way ANOVA.

analysis (absolute area%). Analytes were separated using a Restek Pinnacle-C18 (4.6 mm × 50 mm, 5 μm particle size) column with gradient elution of water and methanol (0.1% formic acid) at a flow rate of 0.8 mL min^{-1}. To determine purity of the compounds, blank UV chromatograms were subtracted from sample UV chromatograms and the blank subtracted chromatograms were integrated. The optical purity was determined with an Agilent 1100 HPLC system using a DAD detector. The mobile phase consisted of high-performance liquid chromatography (HPLC) grade ethanol and *n*-hexane and the stationary phase was a Pirkle Whelk-01 column (4.6 mm × 25 cm × 5 μm particle size).

4.1 General procedures and compound characterization

2 mL of anhydrous toluene was added to a 10 mL 1-neck round bottom flask and degassed by bubbling nitrogen gas through the solution. (3*R*)-7-Bromo-5-(2-fluorophenyl)-3-methyl-1,3-dihydro-2*H*-1,4-benzodiazepin-2-one (**1**) (0.1736 g, 0.5 mmol) was added, followed by the addition of amine (0.6 mmol), $Pd_2(dba)_3$ (0.0229 g, 0.025 mmol), XPhos (0.0238 g, 0.05 mmol) and potassium *t*-butoxide (700 μL, 0.7 mmol, 1 M solution in THF). The solution was stirred at 90 °C under a N_2 atmosphere, while being monitored by TLC (50% ethyl acetate : hexanes) for consumption of the starting material. Once deemed complete by TLC, the solution was cooled to room temperature, filtered through celite and washed with acetone (10 mL). The filtrate was concentrated under reduced pressure to yield a brown residue. The residue was dissolved in acetone and loaded onto a pre-column before being separated by Biotage: 7–7% acetone : hexanes (4 CVs), 7–60% acetone : hexanes (25 CVs) then 60–60% acetone : hexanes (4 CVs). The fractions containing the product were pooled together and concentrated to dryness to yield the desired product.

Compound 2. 7-Anilino-5-(2-fluorophenyl)-3-methyl-1,3-dihydro-2*H*-1,4-benzodiazepin-2-one was obtained as a yellow solid, yield 0.1563 g, 87%. ^{1}H NMR (400 MHz, DMSO) δ 10.41 (s, 1H), 8.21 (s, 1H), 7.57–7.51 (m, J = 3.4 Hz, 2H), 7.33–7.25 (m, J = 2.5 Hz, 3H), 7.13 (q, J = 5.8 Hz, 3H), 6.90 (q, J = 3.2 Hz, 2H), 6.76 (q, J = 5.6 Hz, 2H), 3.71 (q, J = 6.4 Hz, 1H), 1.53 (d, J = 6.4 Hz, 3H). ^{13}C NMR (101 MHz, DMSO) δ 170.69 (s, 1C), 164.67 (s, 1C), 161.4 (s, 1C), 158.93 (s, 1C), 143.67 (s, 1C), 139.10 (s, 1C), 132.38 (d, J = 8.5 Hz, 1C), 132.04 (s, 1C), 131.43 (s, 1C), 129.60 (s, 1C), 129.04 (s, 1C), 128.20 (s, 1C), 128.07 (s, 1C), 125.02 (s, 1C), 122.69 (s, 1C), 121.62 (s, 1C), 120.21 (s, 1C), 116.53 (t, J = 5.0 Hz, 1C), 116.27 (s, 1C), 59.12 (s, 1C), 17.73 (s, 1C). HRMS (ESI/Q-TOF): m/z $[M + H]^+$ pred. for $C_{22}H_{18}N_3OF$: 360.15067; meas.: 360.15046. HPLC purity: 98.76%. Optical purity: 1.4% ee.

Compound 3. 5-(2-Fluorophenyl)-3-methyl-7-(4-methylanilino)-1,3-dihydro-2*H*-1,4-benzodiazepin-2-one was obtained as a pale yellow solid, yield 0.1452 g, 78%. ^{1}H NMR (400 MHz, DMSO) δ 10.37 (s, 1H), 8.08 (s, 1H), 7.51–7.52 (m, J = 2.1 Hz, 2H), 7.33–7.24 (m, J = 3.9 Hz, 2H), 7.20 (q, J = 3.8 Hz, 1H), 7.09 (d, J = 8.8 Hz, 1H), 6.95 (d, J = 8.2 Hz, 2H), 6.82 (d, J = 8.4 Hz, 2H), 6.74 (d, J = 2.5 Hz, 1H), 3.70 (q, J = 6.4 Hz, 1H), 2.18 (s, 3H), 1.53 (d, J = 6.4 Hz, 3H). ^{13}C NMR (101 MHz, DMSO) δ 170.67 (s, 1C), 164.70 (s, 1C), 161.40 (s, 1C), 158.93 (s, 1C), 140.90 (s, 1C), 139.74 (s, 1C), 139.74 (s, 1C), 132.36 (d,

J = 9.2 Hz, 1C), 132.03 (s, 1C), 130.91 (s, 1C), 130.01 (s, 1C), 129.28 (s, 1C), 129.06 (s, 1C), 128.23 (s, 1C), 128.10 (s, 1C), 124.99 (d, *J* = 3.2 Hz, 1C), 122.67 (s, 1C), 120.88 (s, 1C), 117.27 (s, 1C), 116.48 (s, 1C), 116.26 (s, 1C), 115.53 (s, 1C), 59.10 (s, 1C), 59.10 (s, 1C), 20.69 (s, 1C), 17.73 (s, 1C). HRMS (ESI/Q-TOF): *m*/*z* $[M + H]^+$ pred. for $C_{23}H_{20}N_3OF$: 374.16632; meas.: 374.16600. HPLC purity: 97.52 optical purity: 0.8% ee.

Compound 4. 5-(2-Fluorophenyl)-7-(4-methoxyanilino)-3-methyl-1,3-dihydro-2*H*-1,4-benzodiazepin-2-one was obtained as a brown solid, yield 0.1572 g, 81%. ^{1}H NMR (400 MHz, DMSO) *δ* 10.32 (s, 1H), 7.92 (s, 1H), 7.53 (t, *J* = 6.9 Hz, 2H), 7.32–7.24 (m, *J* = 3.1 Hz, 2H), 7.12 (q, *J* = 3.8 Hz, 1H), 7.06 (d, *J* = 8.8 Hz, 1H) 6.89 (q, *J* = 3.0 Hz, 2H), 6.76 (q, *J* = 3.0 Hz, 2H), 6.64 (d, *J* = 2.5 Hz, 1H), 3.67 (s, 4H), 1.52 (d, *J* = 8.8 Hz, 3H). ^{13}C NMR (101 MHz, DMSO) *δ* 170.64 (s, 1C), 164.74 (s, 1C), 161.40 (s, 1C), 158.92 (s, 1C), 154.22 (s, 1C), 140.85 (s, 1C), 136.38 (s, 1C), 132.31 (d, *J* = 8.5 Hz, 1C), 132.02 (s, 1C), 130.36 (s, 1C), 129.13 (s, 1C) 128.19 (d, *J* = 12.9 Hz, 1C), 124.96 (s, 1C), 122.68 (s, 1C), 120.04 (s, 1C), 119.72 (s, 1C), 116.48 (s, 1C), 116.27 (s, 1C), 114.96 (s, 1C), 114.46 (s, 1C), 59.08 (s, 1C), 55.66 (s, 1C), 17.74 (s, 1C). HRMS (ESI/Q-TOF): *m*/*z* $[M + H]^+$ pred. for $C_{23}H_{20}N_3O_2F$: 390.16123; meas.: 390.16090. HPLC purity: 98.59%. Optical purity: 1.2% ee.

Compound 5. 7-(4-Chloroanilino)-5-(2-fluorophenyl)-3-methyl-1,3-dihydro-2*H*-1,4-benzodiazepin-2-one was obtained as a pink solid, yield 0.1472 g, 75%. ^{1}H NMR (400 MHz, DMSO) *δ* 10.45 (s, 1H), 8.34 (s, 1H), 7.57–7.62 (m, *J* = 2.8 Hz, 2H), 7.33–7.25 (m, *J* = 2.7 Hz, 3H), 7.15 (q, *J* = 5.7 Hz, 3H), 6.90 (q, *J* = 3.0 Hz, 2H), 6.77 (d, *J* = 2.5 Hz, 1H), 3.71 (q, *J* = 6.4 Hz, 1H), 1.54 (d, *J* = 6.4 Hz, 3H). ^{13}C NMR (101 MHz, DMSO) *δ* 170.71 (s, 1C), 164.57 (s, 1C), 161.39 (s, 1C), 158.92 (s, 1C), 142.89 (s, 1C), 138.42 (s, 1C), 132.46 (d, *J* = 8.5 Hz, 1C), 132.01 (d, *J* = 8.0 Hz, 1C), 129.40 (s, 1C), 129.05 (s, 1C), 128.11 (s, 1C), 127.9 (s, 1C), 125.03 (s, 1C), 123.14 (s, 1C), 122.75 (s, 1C), 122.11 (s, 1C), 117.64 (s, 1C), 117.28 (s, 1C), 116.53 (s, 1C), 116.31 (s, 1C), 59.13 (s, 1C), 17.72 (s, 1C). HRMS (ESI/Q-TOF): *m*/*z* $[M + H]^+$ pred. for $C_{22}H_{17}N_3OFCl$: 394.11169; meas.: 394.11145. HPLC purity: 98.64%. Optical purity: 1.8% ee.

Compound 6. 5-(2-Fluorophenyl)-3-methyl-7-(4-nitroanilino)-1,3-dihydro-2*H*-1,4-benzodiazepin-2-one was obtained as an orange solid, yield 0.1695 g, 84%. ^{1}H NMR (400 MHz DMSO) *δ* 10.67 (s, 1H), 9.28 (s, 1H), 8.06 (q, *J* = 3.3 Hz, 1H), 7.59–7.49 (m, *J* = 3.6 Hz, 3H), 7.47–7.43 (m, *J* = 4.2 Hz, 1H), 7.32–7.25 (m, *J* = 5.8 Hz, 3H), 7.06 (d, *J* = 8.0 Hz, 2H), 6.85 (t, *J* = 7.4 Hz, 1H), 3.75 (q, *J* = 6.4 Hz, 1H), 1.56 (d, *J* = 6.4 Hz, 3H). ^{13}C NMR (101 MHz, DMSO) *δ* 170.84 (s, 1C), 164.34 (s, 1C), 158.94 (s, 1C), 151.07 (s, 1C), 138.56 (s, 1C), 135.54 (s, 1C), 134.37 (s, 1C), 132.63 (d, *J* = 8.4 Hz, 1C), 132.10 (s, 1C), 129.03 (s, 1C), 127.91 (s, 1C), 127.78 (s, 1C), 126.58 (s, 1C), 125.16 (d, *J* = 6.3 Hz, 1C), 122.87 (s, 1C), 121.13 (s, 1C), 116.58 (s, 1C), 116.37 (s, 1C), 113.57 (s, 1C), 59.21 (s, 1C), 17.68 (s, 1C). HRMS (ESI/Q-TOF): *m*/*z* $[M + H]^+$ pred. for $C_{22}H_{17}N_4O_3F$: 405.13575; meas.: 405.13538. HPLC purity: 93.80%. Optical purity: 2.0% ee.

Compound 7. 5-(2-Fluorophenyl)-3-methyl-7-((4-(methylthio)-phenyl)amino)-1,3-dihydro-2*H*-1,4-benzodiazepin-2-one was obtained as an off-white solid, yield 0.1173 g, 58%. ^{1}H NMR (400 MHz DMSO) *δ* 10.41 (s, 1H), 8.24 (s, 1H), 7.57–7.52 (m, *J* = 3.3 Hz, 2H), 7.33–7.23 (m, *J* = 3.3 Hz, 3H), 7.13–7.09 (m, *J* = 2.9 Hz, 3H), 6.88 (q, *J* = 2.9 Hz, 2H), 6.75 (d, *J* = 2.5 Hz, 1H), 3.70 (q, *J* = 6.4 Hz, 1H), 2.38 (s, 3H), 1.53 (d, *J* = 6.4 Hz, 3H). ^{13}C NMR (101 MHz, DMSO) *δ* 170.69 (s, 1C), 164.63 (s, 1C), 141.81 (s, 1C), 138.96 (s, 1C), 132.46 (s, 1C), 132.07 (s, 1C), 131.50 (s, 1C), 129.55 (s, 1C), 129.06 (s, 1C), 128.04 (s, 1C), 127.56 (s, 1C), 125.01 (s, 1C), 122.71 (s, 1C), 121. 54 (s, 1C), 117.37 (s, 1C), 116.56 (d, *J* = 8.5 Hz, 1C), 116.30 (s, 1C), 59.12 (s, 1C), 17.73 (s, 1C), 17.20 (s, 1C). HRMS (ESI/Q-TOF): *m*/*z* $[M + H]^+$ pred. for $C_{23}H_{20}N_3OFS$: 406.13839; meas.: 406.13854. HPLC purity: 98.40%. Optical purity: 0.2% ee.

Compound 8. 5-(2-Fluorophenyl)-7-(4-methanesulfonylanilino)-3-methyl-1,3-dihydro-2*H*-1,4-benzodiazepin-2-one was obtained as a pale-yellow solid, yield 0.1751 g, 80%. ^{1}H NMR (400 MHz, DMSO) *δ* 10.57 (s, 1H), 8.90 (s, 1H), 7.63–7.53 (m, *J* = 4.6 Hz, 4H), 7.41 (q, *J* = 3.7 Hz, 1H), 7.35–7.26 (m, *J* = 4.8 Hz, 2H), 7.22 (d, *J* = 8.8 Hz, 1H), 6.98 (d, *J* = 8.8 Hz, 2H), 6.89 (d, *J* = 2.4 Hz, 1H), 3.74 (q, *J* = 6.4 Hz, 1H), 3.08 (s, 3H), 1.55 (d, *J* = 6.4 Hz, 3H). ^{13}C NMR (101 MHz, DMSO) *δ* 170.82 (s, 1C), 164.43 (s, 1C), 161.41 (s, 1C), 158.94 (s, 1C), 149.02 (s, 1C), 136.48 (s, 1C), 133.54 (s, 1C), 132.61 (s, 1C), 132.10 (s, 1C), 130.00 (s, 1C), 129.36 (s, 1C), 129.04 (s, 1C), 127.93 (d, *J* = 12.6 Hz, 1C), 125.10 (d, *J* = 3.2 Hz, 1C), 124.29 (s, 1C), 122.81 (s, 1C), 119.99 (s, 1C), 116.55 (s, 1C), 116.34 (s, 1C), 114.13 (s, 1C), 59.18 (s, 1C), 44.63 (s, 1C), 17.69 (s, 1C). HRMS (ESI/Q-TOF): *m*/*z* $[M + H]^+$ pred. for $C_{23}H_{20}N_3O_3FS$: 438.12822; meas.: 438.12834. HPLC purity: 99.07%. Optical purity: 44.8% ee.

Compound 9. 7-(4-Cyanoanilino)-5-(2-fluorophenyl)-3-methyl-1,3-dihydro-2*H*-1,4-benzodiazepin-2-one was obtained as a pale-yellow solid, yield 0.1713 g, 89%. ^{1}H NMR (400 MHz, DMSO) *δ* 10.57 (s, 1H), 8.91 (s, 1H), 7.59–7.51 (m, *J* = 3.1 Hz, 4H), 7.39 (q, *J* = 3.8 Hz, 1H), 7.34–7.26 (m, *J* = 3.5 Hz, 2H), 7.22 (d, *J* = 8.7 Hz, 1H), 6.92 (q, *J* = 3.0 Hz, 2H), 6.87 (d, *J* = 2.4 Hz, 1H), 3.73 (q, *J* = 6.4 Hz, 1H), 1.55 (d, *J* = 6.4 Hz, 3H). ^{13}C NMR (101 MHz, DMSO) *δ* 170.81 (s, 1C), 164.41 (s, 1C), 161.39 (s, 1C), 158.29 (s, 1C), 148.65 (s, 1C), 136.19 (s, 1C), 134.12 (s, 1C), 133.69 (s, 1C), 132.60 (d, *J* = 8.3 Hz, 1C), 132.11 (s, 1C), 129.00 (s, 1C), 127.96 (s, 1C), 127.83 (s, 1C), 125.10 (d, *J* = 3.2 Hz, 1C), 124.50 (s, 1C), 122.82 (s, 1C), 120.27 (d, *J* = 5.5 Hz, 1C), 116.57 (s, 1C), 116.35 (s, 1C), 114.64 (s, 1C), 99.79 (s, 1C), 59.18 (s, 1C), 17.69 (s, 1C). HRMS (ESI/Q-TOF): *m*/*z* $[M + H]^+$ pred. for $C_{23}H_{17}N_4OF$: 385.14592; meas.: 385.14586. HPLC purity: 98.42%. Optical purity: 0.6% ee.

Compound 10. 5-(2-Fluorophenyl)-7-((4-hydroxyphenyl)amino)-3-methyl-1,3-dihydro-2*H*-1,4-benzodiazepin-2-one was obtained as a brown solid, yield 0.0432 g, 23%. ^{1}H NMR (400 MHz, DMSO) *δ* 10.28 (s, 1H), 8.98 (s, 1H), 7.77 (s, 1H), 7.52 (t, *J* = 7.0 Hz, 2H), 7.32–7.22 (m, *J* = 8.3 Hz, 2H), 7.04 (q, *J* = 5.0 Hz, 2H), 6.78 (d, *J* = 8.7 Hz, 2H), 6.59 (q, *J* = 2.9 Hz, 3H), 3.67 (q, *J* = 6.4 Hz, 1H), 1.52 (d, *J* = 6.4 Hz, 3H). ^{13}C NMR (101 MHz, DMSO) *δ* 170.61 (s, 1C), 164.79 (s, 1C), 161.39 (s, 1C), 158.92 (s, 1C), 152.50 (s, 1C), 141.54 (s, 1C), 134.53 (s, 1C), 132.26 (d, *J* = 8.4 Hz, 1C), 132.01 (s, 1C), 129.90 (s, 1C), 129.13 (s, 1C),

128.30 (s, 1C), 128.17 (s, 1C), 124.95 (s, 1C), 122.65 (s, 1C), 119.20 (s, 1C), 116.44 (s, 1C), 116.22 (s, 1C), 116.14 (s, 1C), 113.65 (s, 1C), 59.05 (s, 1C), 17.74 (s, 1C). HRMS (ESI/Q-TOF): *m*/*z* [M + H]$^+$ pred. for $C_{22}H_{18}N_3O_2F$: 376.14588; meas.: 376.14640 HPLC purity: 99.91%. Optical purity 76.4% ee.

Compound 11. 5-(2-Fluorophenyl)-7-(4-methoxycarbonylanilino)-3-methyl-1,3-dihydro-2*H*-1,4-benzodiazepin-2-one was obtained as a pale-yellow solid, yield 0.1351 g, 65%. ^{1}H NMR (400 MHz, DMSO) δ 10.54 (s, 1H), 8.81 (s, 1H), 7.72 (q, *J* = 2.9 Hz, 2H), 7.58–7.53 (m, *J* = 5.3 Hz, 2H), 7.39 (q, *J* = 3.8 Hz, 1H), 7.34–7.26 (m, *J* = 3.1 Hz, 2H), 7.20 (d, *J* = 8.8 Hz, 1H), 6.92–6.88 (m, *J* = 3.4 Hz, 3H), 3.77 (s, 3H), 3.73 (d, *J* = 6.4 Hz, 1H), 1.55 (d, *J* = 6.4 Hz, 3H). ^{13}C NMR (101 MHz, DMSO) δ 170.79 (s, 1C), 166.38 (s, 1C), 164.48 (s, 1C), 161.40 (s, 1C), 158.93 (s, 1C), 148.79 (s, 1C), 136.83 (s, 1C), 133.19 (s, 1C), 132.52 (d, *J* = 8.4 Hz, 1C), 132.08 (d, *J* = 2.5 Hz, 1C), 131.46 (s, 1C), 128.99 (s, 1C), 127.99 (d, *J* = 12.8 Hz, 1C), 125.07 (d, *J* = 3.1 Hz, 1C), 123.99 (s, 1C), 122.77 (s, 1C), 119.73 (s, 1C), 119.43 (s, 1C), 116.52 (s, 1C), 116.31 (s, 1C), 114.11 (s, 1C), 59.17 (s, 1C), 17.70 (s, 1C). HRMS (ESI/Q-TOF): *m*/*z* [M + H]$^+$ pred. for $C_{24}H_{20}N_3O_3F$: 418.15615; meas.: 418.15618 HPLC purity: 99.23%. Optical purity: 1.4% ee.

Compound 12. 5-(2-Fluorophenyl)-7-(4-trifluoromethylanilino)-3-methyl-1,3-dihydro-2*H*-1,4-benzodiazepin-2-one was obtained as a pale-yellow solid, yield 0.1376 g, 64%. ^{1}H NMR (400 MHz, DMSO) δ 10.53 (s, 1H), 8.72 (s, 1H), 7.59–7.62 (m, *J* = 3.4 Hz, 2H), 7.44 (d, *J* = 8.6 Hz, 2H), 7.39 (d, *J* = 3.8 Hz, 1H), 7.32–7.29 (m, *J* = 3.4 Hz, 2H), 7.20 (d, *J* = 8.8 Hz, 1H), 6.99 (d, *J* = 8.5 Hz, 2H), 6.86 (d, *J* = 2.5 Hz, 1H), 3.73 (q, *J* = 6.4 Hz, 1H), 1.55 (d, *J* = 6.4 Hz, 3H). ^{13}C NMR (101 MHz, DMSO) δ 170.79 (s, 1C), 164.48 (s, 1C), 161.41 (s, 1C), 158.94 (s, 1C), 147.85 (s, 1C), 137.05 (s, 1C), 133.08 (s, 1C), 132.52 (d, *J* = 8.3 Hz, 1C), 132.09 (d, *J* = 2.6 Hz, 1C), 129.04 (s, 1C), 127.97 (d, *J* = 12.8 Hz, 1C), 126.96 (d, *J* = 3.8 Hz, 1C), 125.07 (d, *J* = 3.2 Hz, 1C), 123.95 (s, 1C), 123.71 (s, 1C), 122.77 (s, 1C), 119.27 (d, *J* = 3.2 Hz, 1C), 118.93 (s, 1C), 116.55 (s, 1C), 116.33 (s, 1C), 114.67 (s, 1C), 59.17 (s, 1C), 17.70 (s, 1C). HRMS (ESI/Q-TOF): *m*/*z* [M + H]$^+$ pred. for $C_{23}H_{17}N_3OF_4$: 428.13805; meas.: 428.13758. HPLC purity: 96.42%. Optical purity: 0.4% ee.

Compound 13. 7-(2-Cyanoanilino)-5-(2-fluorophenyl)-3-methyl-1,3-dihydro-2*H*-1,4-benzodiazepin-2-one was obtained as a pale yellow solid, yield 0.0965 g, 50%. ^{1}H NMR (400 MHz, DMSO) δ 10.52 (s, 1H), 8.53 (s, 1H), 7.61 (q, *J* = 3.1 Hz, 1H), 7.57–7.52 (m, *J* = 2.5 Hz, 2H), 7.44–7.40 (m, *J* = 2.9 Hz, 1H), 7.37–7.25 (m, *J* = 3.7 Hz, 3H), 7.17 (d, *J* = 8.8 Hz, 1H), 7.10 (d, *J* = 8.4 Hz, 1H), 6.95–6.91 (m, *J* = 3.0 Hz, 2H), 3.72 (q, *J* = 6.4 Hz, 1H), 1.54 (d, *J* = 6.4 Hz, 3H). ^{13}C NMR (101 MHz, DMSO) δ 170.81 (s, 1C), 164.52 (s, 1C), 161.42 (s, 1C), 158.95 (s, 1C), 147.34 (s, 1C), 137.41 (s, 1C), 134.51 (d, *J* = 13.9 Hz, 1C), 133.27 (d, *J* = 8.2 Hz, 1C), 132.07 (s, 1C), 129.03 (s, 1C), 127.97 (d, *J* = 12.8 Hz, 1C), 125.00 (s, 1C), 123.85 (s, 1C), 122.64 (s, 1C), 120.93 (s, 1C), 119.63 (s, 1C), 118.07 (s, 1C), 116.78 (s, 1C), 116.32 (s, 1C), 100.76 (s, 1C), 59.15 (s, 1C), 17.70 (s, 1C). HRMS (ESI/Q-TOF): *m*/*z* [M + H]$^+$ pred. for $C_{23}H_{17}N_4OF$: 385.14592; meas.: 385.14619. HPLC purity: 98.61%. Optical purity: 0.4% ee.

Compound 14. 7-(2-Fluoroanilino)-5-(2-fluorophenyl)-3-methyl-1,3-dihydro-2*H*-1,4-benzodiazepin-2-one obtained as a pale yellow solid, yield 0.0856 g, 45%. ^{1}H NMR (400 MHz, DMSO) δ 10.41 (s, 1H), 8.02 (s, 1H), 7.56–7.51 (m, *J* = 2.1 Hz, 2H), 7.32–7.19 (m, *J* = 4.3 Hz, 3H), 7.15–7.09 (m, *J* = 5.1 Hz, 3H), 6.99–6.95 (m, *J* = 3.3 Hz, 1H), 6.88–6.84 (m, *J* = 2.1 Hz, 1H), 6.76 (d, *J* = 2.4 Hz, 1H), 3.70 (q, *J* = 6.4 Hz, 1H), 1.53 (d, *J* = 6.4 Hz, 3H). ^{13}C NMR (101 MHz, DMSO) δ 170.73 (s, 1C), 164.67 (s, 1C), 161.41 (s, 1C), 154.89 (s, 1C), 152.48 (s, 1C), 138.91 (d, *J* = 8.3 Hz, 1C), 132.04 (s, 1C), 131.42 (d, *J* = 11.2 Hz, 1C), 128.96 (s, 1C), 128.15 (s, 1C), 128.02 (s, 1C), 124.99 (d, *J* = 4.2 Hz, 1C), 122.54 (s, 1C), 121.72 (d, *J* = 10.3 Hz, 1C), 118.92 (s, 1C), 116.83 (s, 1C), 116.44 (d, *J* = 7.4 Hz, 1C), 116.21 (s, 1C), 59.10 (s, 1C), 17.72 (s, 1C). HRMS (ESI/Q-TOF): *m*/*z* [M + H]$^+$ pred. for $C_{22}H_{17}N_3OF_2$: 378.14124; meas.: 378.14283. HPLC purity: 99.98%. Optical purity: 4.4% ee.

Compound 15. 5-(2-Fluorophenyl)-7-((2-trifluoromethyl)-phenyl)amino-3-methyl-1,3-dihydro-2*H*-1,4-benzodiazepin-2-one was obtained as a pale yellow solid, yield 0.1027 g, 48%. ^{1}H NMR (400 MHz, DMSO) δ 10.46 (s, 1H), 7.59–7.50 (m, *J* = 4.3 Hz, 4H), 7.42 (t, *J* = 7.7 Hz, 1H), 7.18 (d, *J* = 8.3 Hz, 3H) 7.12 (d, *J* = 8.7 Hz, 1H), 7.04 (t, *J* = 7.6 Hz, 1H), 6.82 (d, *J* = 2.5 Hz, 1H), 3.71 (q, *J* = 6.4 Hz, 1H), 1.53 (d, *J* = 6.4 Hz, 3H). ^{13}C NMR (101 MHz, DMSO) δ 170.79 (s, 1C), 164.57 (s, 1C), 158.97 (s, 1C), 142.37 (s, 1C), 139.35 (s, 1C), 132.40 (d, *J* = 6.2 Hz, 1C), 132.07 (s, 1C), 129.00 (s, 1C), 128.07 (s, 1C), 127.39 (s, 1C), 124.99 (s, 1C), 123.32 (s, 1C), 122.61 (s, 1C), 121.80 (s, 1C), 121.12 (s, 1C), 119.74 (s, 1C), 119.45 (s, 1C), 118.61 (s, 1C), 116.49 (s, 1C), 116.28 (s, 1C), 59.11 (s, 1C), 17.70 (s, 1C). HRMS (ESI/Q-TOF): *m*/*z* [M + H]$^+$ pred. for $C_{23}H_{17}N_3OF_4$: 428.13805; meas.: 428.13856. HPLC purity: 99.39%. Optical purity: 0.8% ee.

Compound 16. 7-(2-Ethylanilino)-5-(2-fluorophenyl)-3-methyl-1,3-dihydro-2*H*-1,4-benzodiazepin-2-one was obtained as a pale-yellow solid, yield 0.1320 g, 56%. ^{1}H NMR (400 MHz, DMSO) δ 10.33 (s, 1H), 7.53–7.49 (m, *J* = 3.8 Hz, 2H), 7.44 (s, 1H), 7.30–7.23 (m, *J* = 4.2 Hz, 2H), 7.13 (d, *J* = 7.4 Hz, 1H), 7.07 (t, *J* = 2.2 Hz, 2H), 7.00 (t, *J* = 2.1 Hz, 2H), 6.89 (q, *J* = 4.2 Hz, 1H), 6.60 (d, *J* = 2.0 Hz, 1H), 3.68 (q, *J* = 6.4 Hz, 1H), 1.52 (d, *J* = 6.4 Hz, 3H), 1.07 (t, *J* = 7.5 Hz, 3H). ^{13}C NMR (101 MHz, DMSO) δ 170.69 (s, 1C), 164.75 (s, 1C), 158.94 (s, 1C), 141.40 (s, 1C), 140.86 (s, 1C), 135.98 (s, 1C), 132.29 (d, *J* = 8.9 Hz, 1C), 132.03 (s, 1C), 130.58 (s, 1C), 129.38 (s, 1C), 129.05 (s, 1C), 126.75 (s, 1C), 124.94 (s, 1C), 122.89 (s, 1C), 122.56 (s, 1C), 120.68 (s, 1C), 120.40 (s, 1C), 116.45 (s, 1C), 116.24 (s, 1C), 115.18 (s, 1C), 59.06 (s, 1C), 24.00 (s, 1C), 17.72 (s, 1C), 14.47 (s, 1C). HRMS (ESI/Q-TOF): *m*/*z* [M + H]$^+$ pred. for $C_{24}H_{22}N_3OF$: 388.18197; meas.: 388.18301. HPLC purity: 87.07%. Optical purity: 9.8% ee.

Compound 17. 5-(2-Fluorophenyl)-7-(2-methoxyanilino)-3-methyl-1,3-dihydro-2*H*-1,4-benzodiazepin-2-one product was obtained as a pale-yellow solid, yield 0.1537 g, 79%. ^{1}H NMR (400 MHz, DMSO) δ 10.36 (s, 1H), 7.55–7.49 (m, *J* = 3.6 Hz, 3H), 7.31–7.21 (m, *J* = 3.3 Hz, 3H), 7.07 (d, *J* = 8.8 Hz, 1H),

6.99 (q, J = 3.1 Hz, 1H), 6.93 (q, J = 3.1 Hz, 1H), 6.84–6.77 (m, J = 4.0 Hz, 2H), 6.74–6.89 (m, J = 3.3 Hz, 1H), 3.74 (s, 3H), 3.68 (q, J = 6.4 Hz, 1H), 1.52 (d, J = 6.4 Hz, 3H). ^{13}C NMR (101 MHz, DMSO) δ 170.71 (s, 1C), 164.80 (s, 1C), 161.40 (s, 1C), 158.93 (s, 1C), 150.02 (s, 1C), 139.65 (s, 1C), 132.28 (t, J = 6.7 Hz, 1C), 132.00 (s, 1C), 131.08 (s, 1C), 128.90 (s, 1C), 128.27 (s, 1C), 128.14 (s, 1C), 124.93 (d, J = 3.2 Hz, 1C), 122.39 (s, 1C), 121.73 (s, 1C), 121.49 (s, 1C), 120.85 (s, 1C), 116.71 (s, 1C), 116.36 (t, J = 10.8 Hz, 1C), 111.93 (s, 1C), 59.07 (s, 1C), 55.80 (s, 1C), 17.73 (s, 1C). HRMS (ESI/Q-TOF): m/z $[M + H]^+$ pred. for $C_{23}H_{20}N_3O_2F$: 390.16123; meas.: 390.16229. HPLC purity: 100%. Optical purity: 0.2% ee.

Compound 18. 5-(2-Fluorophenyl)-3-methyl-7-(3-methylanilino)-1,3-dihydro-2*H*-1,4-benzodiazepin-2-one was obtained as a pale-yellow solid, yield 0.1275 g, 68%. ^{1}H NMR (400 MHz, DMSO) δ 10.40 (s, 1H), 8.15 (s, 1H), 7.56–7.52 (m, J = 2.1 Hz, 2H), 7.33–7.21 (m, J = 2.7 Hz, 3H), 7.11 (d, J = 8.8 Hz, 1H), 7.01 (t, J = 7.7 Hz, 1H), 6.80 (d, J = 2.5 Hz, 1H), 6.69 (d, J = 8.1 Hz, 2H), 6.58 (d, J = 7.4 Hz, 1H), 3.69 (q, J = 6.4 Hz, 1H), 2.14 (s, 3H), 1.53 (d, J = 6.4 Hz, 3H). ^{13}C NMR (101 MHz, DMSO) δ 170.68 (s, 1C), 164.71 (s, 1C), 143.52 (s, 1C), 139.21 (s, 1C), 138.74 (s, 1C),132.39 (s, 1C), 132.06 (s, 1C), 131.31 (s, 1C), 129.48 (s, 1C), 128.98 (s, 1C), 128.13 (s, 1C), 125.00 (s, 1C), 122.73 (s, 1C), 121.79 (s, 1C), 121.09 (s, 1C), 116.98 (s, 1C), 116.49 (s, 1C), 116.28 (s, 1C), 116.06 (s, 1C), 114.13 (s, 1C), 59.11 (s, 1C), 21.67 (s, 1C), 17.74 (s, 1C). HRMS (ESI/Q-TOF): m/z $[M + H]^+$ pred. for $C_{23}H_{20}N_3OF$: 374.16632; meas.: 374.16747. HPLC purity: 99.61%. Optical purity: 2.0% ee.

Compound 19. 7-(3-Cyanoanilino)-5-(2-fluorophenyl)-3-methyl-1,3-dihydro-2*H*-1,4-benzodiazepin-2-one was obtained as a pale-yellow solid, yield 0.1087 g, 57%. ^{1}H NMR (400 MHz, DMSO) δ 10.51 (s, 1H), 8.59 (s, 1H), 7.59–7.54 (m, J = 3.0 Hz, 2H), 7.36–7.25 (m, J = 3.5 Hz, 4H), 7.20–7.14 (m, J = 2.8 Hz, 4H), 6.82 (d, J = 2.5 Hz, 1H), 3.74–3.70 (m, J = 4.8 Hz, 1H), 1.54 (d, J = 6.4 Hz, 3H). ^{13}C NMR (101 MHz, DMSO) δ 164.47 (s, 1C), 161.34 (s, 1C), 158.88 (s, 1C), 145.15 (s, 1C), 137.29 (s, 1C), 132.91 (s, 1C), 132.55 (d, J = 8.5 Hz, 1C), 132.12 (s, 1C), 131.02 (s, 1C), 129.04 (s, 1C), 127.95 (d, J = 12.8 Hz, 1C), 125.07 (s, 1C), 123.31 (s, 1C), 122.94 (s, 1C), 120.48 (s, 1C), 119.38 (s, 1C), 118.55 (s, 1C), 117.34 (s, 1C), 116.43 (d, J = 21.4 Hz 1C), 112.47 (s, 1C), 59.15 (s, 1C), 17.71 (s, 1C). HRMS (ESI/Q-TOF): m/z $[M + H]^+$ pred. for $C_{23}H_{17}N_4OF$: 385.14592; meas.: 384.14687. HPLC purity: 99.28%. Optical purity: 0.4% ee.

Compound 20. 5-(2-Fluorophenyl)-7-(2,4-dimethylanilino)-3-methyl-1,3-dihydro-2*H*-1,4-benzodiazepin-2-one was obtained as a pale-yellow solid, yield 0.1603 g, 83%. ^{1}H NMR (400 MHz, DMSO) δ 10.30 (s, 1H), 7.55–7.49 (m, J = 2.5 Hz, 2H), 7.37 (s, 1H), 7.31–7.23 (m, J = 3.1 Hz, 2H), 7.03 (t, J = 1.9 Hz, 2H), 6.91 (q, J = 4.8 Hz, 2H), 6.81 (q, J = 3.3 Hz, 1H), 6.56 (d, J = 2.1 Hz, 1H), 3.67 (q, J = 6.4 Hz, 1H), 2.18 (s, 3H), 2.06 (s, 3H), 1.52 (d, J = 6.4 Hz, 3H). ^{13}C NMR (101 MHz, DMSO) δ 170.69 (s, 1C), 164.77 (s, 1C), 161.4 (s, 1C), 158.93 (s, 1C), 141.46 (s, 1C), 138.78 (s, 1C), 132.27 (d, J = 8.3 Hz, 1C), 131.96 (d, J = 12.2 Hz, 1C), 131.49 (s, 1C), 130.27 (s, 1C), 130.13 (s, 1C), 129.09 (s, 1C), 128.20 (d, J = 12.8 Hz, 1C), 127.26 (s, 1C), 124.93 (d, J = 3.1 Hz, 1C), 122.54 (s, 1C), 120.14 (d, J = 4.4 Hz, 1C), 116.45 (s, 1C), 116.24 (s, 1C), 114.68 (s, 1C), 59.05 (s, 1C), 20.78 (s, 1C), 18.17 (s, 1C), 17.72 (s, 1C). HRMS (ESI/Q-TOF): m/z $[M + H]^+$ pred. for $C_{24}H_{24}N_3OF$: 388.18197; meas.: 388.18240. HPLC purity: 95.26%. Optical purity: 1.0% ee.

Compound 21. 5-(2-Fluorophenyl)-7-(*N*-methylanilino)-3-methyl-1,3-dihydro-2*H*-1,4-benzodiazepin-2-one was obtained as a pale-yellow solid, yield 0.0826 g, 44%. ^{1}H NMR (400 MHz, DMSO) δ 10.52 (s, 1H), 7.55–7.47 (m, J = 2.3 Hz, 2H), 7.30–7.23 (m, J = 3.9 Hz, 3H), 7.18 (t, J = 8.2 Hz, 3H), 6.90–6.81 (m, J = 4.5 Hz, 3H), 6.71 (d, J = 2.6 Hz, 1H), 3.71 (q, J = 6.4 Hz, 1H), 3.15 (s, 3H), 1.54 (d, J = 6.4 Hz, 3H). ^{13}C NMR (101 MHz, DMSO) δ 170.8 (s, 1C), 164.54 (s, 1C), 161.41 (s, 1C), 158.94 (s, 1C), 148.55 (s, 1C), 143.92 (s, 1C), 133.03 (s, 1C), 132.50 (d, J = 8.4 Hz, 1C), 132.05 (d, J = 2.5 Hz, 1C), 129.57 (s, 1C), 128.83 (s, 1C), 127.85 (s, 1C), 127.72 (s, 1C), 125.42 (s, 1C), 124.96 (d, J = 3.3 Hz, 1C), 122.86 (s, 1C), 121.07 (d, J = 7.4 Hz, 1C), 119.11 (s, 1C), 116.48 (s, 1C), 116.26 (s, 1C), 59.15 (s, 1C), 31.16 (s, 1C), 17.69 (s, 1C). HRMS (ESI/Q-TOF): m/z $[M + H]^+$ pred. for $C_{23}H_{20}N_3OF$: 374.16632; meas.: 374.16657. HPLC purity: 99.04%. Optical purity: 0.4% ee.

Compound 22. 5-(2-Fluorophenyl)-3-methyl-7-(morpholin-4-yl)-1,3-dihydro-2*H*-1,4-benzodiazepin-2-one was obtained as an off-hite solid, yield 0.1259 g, 71%. ^{1}H NMR (400 MHz, DMSO) δ 10.37(s, 1H), 7.56–7.51 (m, J = 4.1 Hz, 2H), 7.33–7.29 (m, J = 4.0 Hz, 1H), 7.25–7.19 (m, J = 3.9 Hz, 2H), 7.12 (d, J = 9.0 Hz, 1H), 6.53 (d, J = 2.7H, 1H), 3.65 (q, J = 5.3 Hz, 5H), 2.99–2.94 (m, J = 5.4 Hz, 2H), 2.90–2.84 (m, J = 5.4 Hz, 2H), 1.51 (d, J = 6.4 Hz, 3H). ^{13}C NMR (101 MHz, DMSO) δ 170.86 (s, 1C), 164.84 (s, 1C), 161.42 (s, 1C), 158.95 (s, 1C), 146.98 (s, 1C), 132.42 (d, J = 8.5 Hz, 1C), 132.10 (s, 1C), 131.29 (s, 1C), 128.86 (s, 1C), 127.98 (s, 1C), 124.97 (s, 1C), 122.43 (s, 1C), 120.41 (s, 1C), 116.45 (s, 1C), 116.24 (s, 1C), 114.18 (s, 1C), 59.05 (s, 1C), 49.06 (s, 1C), 17.67 (s, 1C). HRMS (ESI/Q-TOF): m/z $[M + H]^+$ pred. for $C_{20}H_{20}N_3O_2F$: 354.16123; meas.: 354.16143. HPLC purity: 93.76%. Optical purity: 0.4% ee.

Compound 23. 5-(2-Fluorophenyl)-3-methyl-7-(piperidin-1-yl)-1,3-dihydro-2*H*-1,4-benzodiazepin-2-one was obtained as a pale-yellow solid, yield 0.113 g, 64%. ^{1}H NMR (400 MHz, DMSO) δ 10.33 (s, 1H), 7.56–7.50 (m, J = 3.4 Hz,2H), 7.33–7.29 (m, J = 3.2 Hz, 1H), 7.24–7.20 (m, J = 4.8 Hz, 2H), 7.08 (d, J = 9.0 Hz 1H), 6.50 (d, J = 2.7 Hz, 1H), 3.64 (q, J = 6. 4 Hz, 1H), 2.96 (q, J = 5.9 Hz, 2H), 2.93–2.87 (m, J = 5.7 Hz, 2H), 1.55–1.50 (m, J = 3.6 Hz, 6H), 1.46 (q, J = 3.4 Hz,3H). ^{13}C NMR (101 MHz, DMSO) δ 170.78 (s, 1C), 164.92 (s, 1C), 161.41 (s, 1C), 158.94 (s, 1C), 147.64 (s, 1C), 132.38 (d, J = 8.4 Hz, 1C), 132.07 (s, 1C), 130.70 (s, 1C), 128.81 (s, 1C), 128.13 (d, J = 12.7 Hz, 1C), 124.92 (s, 1C), 122.34 (s, 1C), 121.32 (s, 1C), 116.42 (s, 1C), 116.20 (s, 1C), 114.80 (s, 1C), 59.05 (s, 1C), 50.24 (s, 1C), 25.50 (s, 1C), 24.07 (s, 1C), 17.69 (s, 1C). HRMS (ESI/Q-TOF): m/z $[M + H]^+$ pred. for $C_{21}H_{22}N_3OF$: 352.18197; meas.: 352.18120. HPLC purity: 91.16%. Optical purity: 0.2% ee.

Compound 24. 7-(Benzylamino)-5-(2-fluorophenyl)-3-methyl-1,3-dihydro-2*H*-1,4-benzodiazepin-2-one was obtained as a pale-yellow solid, yield 0.1075 g, 58%. ^{1}H NMR (400 MHz, DMSO) δ 10.12 (s, 1H), 7.52–7.42 (m, J = 2.3 Hz, 2H), 7.28–7.22 (m, J = 2.8 Hz, 3H), 7.20–7.14 (m, J = 4.5 Hz, 4H), 6.94 (d, J = 8.8 Hz, 1H), 6.80 (q, J = 3.8 Hz, 1H), 6.36 (t, J = 6.0 Hz, 1H), 6.26 (d, J = 2.6 Hz, 1H), 4.10 (q, J = 2.8 Hz, 2H), 3.60 (q, J = 6.4 Hz, 1H), 1.48 (d, J = 6.4 Hz, 3H). ^{13}C NMR (101 MHz, DMSO) δ 170.58 (s, 1C), 165.00 (s, 1C), 144.84 (s, 1C), 140.18 (s, 1C), 132.05 (s, 1C), 131.84 (s, 1C), 129.15 (s, 1C), 128.71 (s, 1C), 128.34 (s, 1C), 128.19 (s, 1C), 127.53 (s, 1C), 127.07 (s, 1C), 124.74 (s, 1C), 122.46 (s, 1C), 117.10 (s, 1C), 116.41 (s, 1C), 116.19 (s, 1C), 110.98 (s, 1C), 47.06 (s, 1C), 17.71 (s, 1C). HRMS (ESI/Q-TOF): m/z [M + H]$^+$ pred. for $C_{23}H_{20}N_3OF$: 374.16632; meas.: 374.16635. HPLC purity: 92.42%. Optical purity: 1.0% ee.

Compound 25. 7-(*tert*-Butylamino)-5-(2-fluorophenyl)-3-methyl-1,3-dihydro-2*H*-1,4-benzodiazepin-2-one was obtained as a yellow solid, yield 0.1209 g, 71%. ^{1}H NMR (400 MHz, DMSO) δ 10.16 (s, 1H), 7.64–7.50 (m, J = 2.8 Hz, 2H), 7.32–7.26 (m, J = 3.2 Hz, 1H), 7.22 (q, J = 6.4 Hz, 1H), 6.93 (s, 2H), 6.42 (d, J = 1.6 Hz, 1H), 5.22 (s, 1H), 3.64 (q, J = 6.4 Hz, 1H), 1.50 (d, J = 6.5 Hz, 3H), 1.13 (s, 9H). ^{13}C NMR (101 MHz, DMSO) δ 170.53 (s, 1C), 165.06 (s, 1C), 158.92 (s, 1C), 143.76 (s, 1C), 132.13 (d, J = 8.3 Hz, 1C), 131.96 (s, 1C), 128.86 (s, 1C), 128.53 (d, J = 4.0 Hz, 1C), 128.38 (s, 1C), 124.87 (d, J = 3.2 Hz, 1C), 122.13 (s, 1C), 120.52 (s, 1C), 116.34 (s, 1C), 116.13 (s, 1C), 114.32 (s, 1C), 59.00 (s, 1C), 50.80 (s, 1C), 29.71 (s, 1C), 17.75 (s, 1C), 14.44 (s, 1C). HRMS (ESI/Q-TOF): m/z [M + H]$^+$ pred. for $C_{20}H_{22}N_3OF$: 340.18197; meas.: 340.18190. HPLC purity: 88.92%. Optical purity: 4.4% ee.

Compound 26. 7-(Cyclohexylamino)-5-(2-fluorophenyl)-3-methyl-1,3-dihydro-2*H*-1,4-benzodiazepin-2-one was obtained as a pale-yellow solid, yield 0.1789 g, 81%. ^{1}H NMR (400 MHz, DMSO) δ 10.11 (s, 1H), 7.52–7.49 (m, J = 5.5 Hz,2H), 7.31–7.28 (m, J = 2.5 Hz, 1H), 7.23–7.20 (m, J = 8.1 Hz, 2H), 6.95 (d, J = 7.0 Hz 1H), 6.79–6.77 (dd, J = 5.1 Hz, 1H), 6.23 (d, J = 2.7 Hz, 1H), 5.51 (d, J = 6.3 Hz, 1H), 3.64 (q, J = 6. 4 Hz, 1H), 2.96 (q, J = 5.9 Hz, 2H), 2.93–2.87 (m, J = 5.7 Hz, 2H), 1.55–1.50 (m, J = 3.6 Hz, 6H), 1.09 (q, J = 3.4 Hz, 3H). ^{13}C NMR (101 MHz, DMSO) δ 170.56 (s, 1C), 165.05 (s, 1C), 161.16 (s, 1C), 159.18 (s, 1C), 144.20 (s, 1C), 132.06 (q, J = 2.4 Hz, 1C), 132.00 (s, 1C), 130.00 (s, 1C), 127.76 (s, 1C), 124.82 (d, J = 2.5 Hz, 1C), 122.52 (s, 1C), 116.79 (s, 1C), 116.32 (s, 1C), 116.15 (s, 1C), 111.30 (s, 1C), 59.95 (s, 1C), 51.11 (s, 1C), 32.74 (d, J = 24.2 Hz, 1C) 25.96 (s, 1C), 24.82 (d, J = 23.2 Hz, 1C), 17.74 (s, 1C). HRMS (ESI/Q-TOF): m/z [M + H]$^+$ pred. for $C_{22}H_{24}N_3OF$: 366.19762; meas.: 366.20045. HPLC purity: 99.14%. Optical purity: 2.2% ee.

Compound 27. 7-(Dimethylamino)-5-(2-fluorophenyl)-3-methyl-1,3-dihydro-2*H*-1,4-benzodiazepin-2-one was obtained as a pale-yellow solid, yield 0.1372 g, 76%. ^{1}H NMR (400 MHz, DMSO) δ 10.24 (s, 1H), 7.56–7.51 (m, J = 4.0 Hz, 2H), 7.32–7.29 (m, J = 4.0 Hz, 1H), 7.22–7.19 (m, J = 6.0 Hz, 2H), 7.07 (d, J = 7.2 Hz 1H), 7.02–7.00 (dd, J = 2.1 Hz, 1H), 6.28 (d, J = 10.5 Hz, 1H), 3.65–3.63 (q, J = 5.2 Hz, 1H), 2.75 (s, 6H), 1.51 (d, J = 5.1 Hz, 3H). ^{13}C NMR (101 MHz, DMSO) δ 170.75 (s, 1C), 165.05 (s, 1C), 161.43 (s, 1C), 159.95 (s, 1C), 146.52 (s, 1C), 132.35 (q, J = 20.8 Hz, 1C), 129.03 (s, 1C), 128.82 (s, 1C), 128.30 (d, J = 12.8 Hz, 1C), 124.90 (d, J = 3.4 Hz, 1C), 122.46 (s, 1C), 117.40 (s, 1C), 116.38 (d, J = 21.7 Hz, 1C) 110.99 (s, 1C), 58.99 (s, 1C), 17.71 (s, 1C). HRMS (ESI/Q-TOF): m/z [M + H]$^+$ pred. for $C_{18}H_{18}N_3OF$: 312.15067; meas.: 312.15246. HPLC purity: 99.25%. Optical purity: 1.8% ee.

4.2 Aqueous solubility assay

2 mg of compound was added to 1 mL of PBS buffer at pH 7.4. The solutions were vortexed for 10 s, sonicated for 2 min and agitated with a horizontal shaker in a closed vial for 24 h. The mixtures were transferred to an Eppendorf tube and centrifuged for 5 min at 16 000 × g followed by filtration through 0.22 μm cellulose acetate spin X centrifuge filter (Costar). 200 μL of filtrate was transferred to a new Eppendorf tube and 300 μL of methanol was added. After mixing, 50 μL were transferred into a 384 well plate (Coring UV star, 781 801) for UV detection at 230–600 nm (Tecan M1000). The assay was carried out with three independent samples of each compound. The concentration of each solution was determined with a calibration curve in 60 : 40 methanol/PBS buffer water. Absorbance of corresponding methanol PBS blank were recorded and subtracted from the absorbance of calibration curve solutions and from the samples.

4.3 Cell viability assay

Human embryonic kidney HEK293T cells were added to each well of a sterile optical bottom 384-well plates (20 μL containing 15 000 cells). Plates were incubated for 4 h at 37 °C followed by the addition of 200 nL of a serial diluted compound using a Tecan Freedom EVO liquid handling system with a 100H stainless steel pin tool. The controls for the cytotoxicity assay were 3-dibutylamino-1-(4-hexyl-phenyl)-propan-1-one (positive) and DMSO (negative). After 18 h, 20 μL of Cell Titer-Glo (Promega, Madison, WI) was added to each well followed by quantification of luminescence using a Tecan Infinite M1000 plate reader. The assay was performed in quadruplicate, and data were analyzed using non-linear regression with variable slope (GraphPrism).

4.4 Receptor binding assay

The ARα_2 radio ligand binding assays were carried out with cell membranes from cells (HEK293 and MDCK) overexpressing specific human ARα_2 subtypes. Cell membranes, ^{3}H-rauwolscinein and compounds were incubated for 90 min absorbed onto a PEI-soaked membrane and combined with scintillation cocktail to enable detected by Microbeta counter.[29] Cell-based β-arrestin recruitment assay was carried out with HTLA (HEK293 cell line stably expressing a tTA-dependent luciferase reporter and a β-arrestin2-TEV fusion gene). HTLA were transfected with

$AR\alpha_2$ subtype tango constructs, followed by the addition of compound for 18 h and Bright-Glo for quantification of luciferase as a measure of β-arrestin recruitment.[30]

4.5 Molecular docking

Available PDB files ($AR\alpha_{2A}$ 6KUX,[32] $AR\alpha_{2B}$ 6K41,[33] and $AR\alpha_{2C}$ 6KUW[34]) were uploaded in MOE (Molecular Operating Environment) and prepared for docking using the structure preparation tool followed by protonate 3D. Next (*S*)-**2** and (*R*)-**2** were drawn and saved as a database file. Next, MOE DOCK was used for docking 2 into the ligand site of the receptors using triangle matcher placement and induced fit refinement. Docking scores were calculated using London dG and GBVI/WSA dG energies.

4.6 Rotarod study

Female Swiss Webster mice, aged ten weeks, were obtained from Charles River Laboratories and kept in a pathogen-free environment with a 12-hour light/dark cycle, with unrestricted food and water access. All studies were conducted in accordance with institutional guidelines as defined by UWM Institutional Animal Care and Use Committee. The approved IACUC number is 23-24 #17. Mice were trained to maintain balance at a constant speed of 15 rpm on the rotarod apparatus (Omnitech Electronics, Inc.) for 3 min. Compounds were dissolved in hot PEG400 (2.5 % v/v) followed by the addition of 2% hydroxypropylmethylcellulose solution (97.5% v/v). Each mouse received a volume of 100 μL by oral gavage. Mice were placed on the rotarod for 3 min at 10, 30, and 60 min after each administration. If a mouse fell before 3 min had elapsed, it was placed again on the rotating rod. If a mouse fell for the second time, the time of the fall was recorded. Data analysis was carried out with GraphPad Prism (GraphPad) using two-way analysis of variance (ANOVA) repeated measures and Bonferroni posttest (n = 8).

4.7 Pharmacokinetic studies

Female Swiss Webster mice, aged ten weeks, were obtained from Charles River Laboratories and kept in a pathogen-free environment with a 12-hour light/dark cycle, with unrestricted food and water access. All studies were conducted in accordance with institutional guidelines as defined by UWM Institutional Animal Care and Use Committee. The approved IACUC number is 22-23 #30. Mice were administered compound **2** at 40 mg kg^{-1} in 100 μL vehicle (95% of a 2% solution of HPMC and 5% of PEG400). Mice were euthanized at the indicated time points followed by isolation of blood and brain. To 100 μL blood aliquots were added to 300 μL of cold acetonitrile and vortexed and sonicated for 30 s followed by centrifugation 7500 × *g* for 10 min. 300 μL of the supernatant was transferred to clean tubes and evaporated using a Speedvac concentrator (ThermoFisher). The residue was reconstituted with 150 μL acetonitrile and spin-filtered through 0.22 μm nylon centrifugal filter units (Costar). LC-MS/MS sample were prepared by combing 90 μL of sample with 10 μL of 10 μmol solution of 4,5-diphenylimidazole. Brains were weighed and homogenized directly in 400 μL cold acetonitrile using a Cole Palmer LabGen 7B homogenizer in a 4 ml glass vial. Samples were centrifuged in same vial for 10 min at 4000 × *g*. 300 μL of the supernatant was transferred to clean tubes and evaporated using a Speedvac concentrator (ThermoFisher). The residue was reconstituted with 150 μL of acetonitrile, sonicated for 30 s and spun down at 7500 × *g*. The supernatant was spin-filtered through 0.22 μm nylon centrifugal filter units (Costar). After reconstitution, 90 μL of this solution was combined with 10 μL of 4,5-diphenylimidazole (10 uM in acetonitrile) for analysis. For analytical method (LCMS/MS) see SI.

4.8 Open field study

The open field test (OFT) is a behavioral assessment tool used to evaluate an animal's exploratory behavior and general activity in a novel, enclosed environment. Ten-week-old female Swiss Webster adult mice were purchased from Charles River Laboratories and housed pathogen-free with a 12 h light and dark cycle. Animals had free access to food and water. All studies were conducted in accordance with institutional guidelines as defined by UWM Institutional Animal Care and Use Committee. The approved IACUC number is 23-24 #17. Compounds were dissolved in hot PEG400 (2.5% v/v) followed by the addition of 2% hydroxypropylmethylcellulose solution (97.5% v/v). Each mouse received a volume of 100 μL by oral gavage. Each animal is placed into the locomotor activity chamber; an open-field acrylic arena with a digital USB camera (Stoelting Co; Cat#10-000-332) attached overhead and behavior is recorded for 3 min. The arena is a 40 cm square box (Stoelting Co; Cat #60100) with a transparent wall and detachable fiber base designed for easy cleaning. Automated video tracking software (ANY-maze Version 7.48) was used to plot their ambulatory and fine motor movements, as well as rearing behavior. The animals are under no motivational constraints and are free to explore the environment. For each trial, total distance travelled, speed, movement time, freezing time, central zone time and tracking plot were derived. The chamber is cleaned with disinfectant in between the testing of each animal. Data analysis was carried out with GraphPad Prism (GraphPad) using independent *t*-test and data are expressed as means ± SEM (n = 6).

Author contributions

MRTF, ABV, SGH, and DAW carried out synthesis, characterization and preclinical analysis. MAT, KMM, and MJM performed cell-based and *in vivo* assays. MRTF and LAA wrote the manuscript with input from all authors. All authors have reviewed and edited the final version of the manuscript. Conceptualization, funding acquisition and project administration were provided by LAA.

Conflicts of interest

We received the 23 phosphorous containing ligands from Millipore Sigma to identify the best ligand for this specific amination reaction.

Data availability

Supplementary information: The SI includes ^{1}H, ^{13}C, mass, and chromatography data for each compound. Futhermore, we included dose response curves for cytotoxicity and receptor binding, rotarod graphs, information for pharmacokinetic analysis, and bar graphs for open field measurments. See DOI: **https://doi.org/10.1039/D5MD00611B**.

The data supporting this article have been included as part of the SI.

Acknowledgements

This work was supported by the National Institutes of Health R41HL147658 (L. A. A.) as well as the University of Wisconsin-Milwaukee, University of Wisconsin-Milwaukee Research Foundation (Catalyst grant), the Lynde and Harry Bradley Foundation, and the Richard and Ethel Herzfeld Foundation. In addition, this work was supported by grant CHE-1625735 from the National Science Foundation. Ki determinations and agonist/antagonist functional data were generously provided by the National Institute of Mental Health's Psychoactive Drug Screening Program, Contract # 75N95023C00021 (NIMH PDSP). The NIMH PDSP is Directed by Bryan L. Roth MD, PhD at the University of North Carolina at Chapel Hill and Project Officer Jamie Driscoll at NIMH, Bethesda MD, USA.

References

1 S. G. Smith, R. Sanchez and M. M. Zhou, Privileged diazepine compounds and their emergence as bromodomain inhibitors, *Chem. Biol.*, 2014, **21**(5), 573–583.
2 C. E. Griffin 3rd, A. M. Kaye, F. R. Bueno and A. D. Kaye, Benzodiazepine pharmacology and central nervous system-mediated effects, *Ochsner J.*, 2013, **13**(2), 214–223.
3 K. Vandyck, M. D. Cummings, O. Nyanguile, C. W. Boutton, S. Vendeville, D. McGowan, B. Devogelaere, K. Amssoms, S. Last, K. Rombauts, A. Tahri, P. Lory, L. Hu, D. A. Beauchamp, K. Simmen and P. Raboisson, Structure-based design of a benzodiazepine scaffold yields a potent allosteric inhibitor of hepatitis C NS5B RNA polymerase, *J. Med. Chem.*, 2009, **52**(14), 4099–4102.
4 C. G. Joseph, K. R. Wilson, M. S. Wood, N. B. Sorenson, D. V. Phan, Z. Xiang, R. M. Witek and C. Haskell-Luevano, The 1,4-benzodiazepine-2,5-dione small molecule template results in melanocortin receptor agonists with nanomolar potencies, *J. Med. Chem.*, 2008, **51**(5), 1423–1431.
5 Y. Huang, S. Wolf, M. Bista, L. Meireles, C. Camacho, T. A. Holak and A. Domling, 1,4-Thienodiazepine-2,5-diones via MCR (I): synthesis, virtual space and p53-Mdm2 activity, *Chem. Biol. Drug Des.*, 2010, **76**(2), 116–129.
6 C. Saunders and L. E. Limbird, Localization and trafficking of alpha2-adrenergic receptor subtypes in cells and tissues, *Pharmacol. Ther.*, 1999, **84**(2), 193–205.
7 M. M. Bucheler, K. Hadamek and L. Hein, Two alpha(2)-adrenergic receptor subtypes, alpha(2A) and alpha(2C), inhibit transmitter release in the brain of gene-targeted mice, *Neuroscience*, 2002, **109**(4), 819–826.
8 K. Chen, Z. Lu, Y. C. Xin, Y. Cai, Y. Chen and S. M. Pan, Alpha-2 agonists for long-term sedation during mechanical ventilation in critically ill patients, *Cochrane Database Syst. Rev.*, 2015, **1**(1), CD010269.
9 L. S. Stone, L. B. MacMillan, K. F. Kitto, L. E. Limbird and G. L. Wilcox, The alpha2a adrenergic receptor subtype mediates spinal analgesia evoked by alpha2 agonists and is necessary for spinal adrenergic-opioid synergy, *J. Neurosci.*, 1997, **17**(18), 7157–7165.
10 L. Gowing, M. Farrell, R. Ali and J. M. White, Alpha(2)-adrenergic agonists for the management of opioid withdrawal, *Cochrane Database Syst. Rev.*, 2016, **2016**(5), CD002024.
11 R. E. Link, K. Desai, L. Hein, M. E. Stevens, A. Chruscinski, D. Bernstein, G. S. Barsh and B. K. Kobilka, Cardiovascular regulation in mice lacking alpha2-adrenergic receptor subtypes b and c, *Science*, 1996, **273**(5276), 803–805.
12 K. P. Makaritsis, C. Johns, L. Gavras and H. Gavras, Role of α-adrenergic receptor subtypes in the acute hypertensive response to hypertonic saline infusion in anephric mice, *Hypertension*, 2000, **35**(2), 609–613.
13 S. Sawamura, W. S. Kingery, M. F. Davies, G. S. Agashe, J. D. Clark, B. K. Kobilka, T. Hashimoto and M. Maze, Antinociceptive action of nitrous oxide is mediated by stimulation of noradrenergic neurons in the brainstem and activation of α-adrenoceptors, *J. Neurosci.*, 2000, **20**(24), 9242–9251.
14 G. T. Mah, A. M. Tejani and V. M. Musini, Methyldopa for primary hypertension, *Cochrane Database Syst. Rev.*, 2009, **2009**(4), CD003893.
15 S. H. Kollins, R. Jain, M. Brams, S. Segal, R. L. Findling, S. B. Wigal and M. Khayrallah, Clonidine extended-release tablets as add-on therapy to psychostimulants in children and adolescents with ADHD, *Pediatrics*, 2011, **127**(6), e1406–e1413.
16 V. M. Musini, P. Pasha and J. M. Wright, Blood pressure lowering efficacy of clonidine for primary hypertension, *Cochrane Database Syst. Rev.*, 2015(3), CD008284.
17 R. Gertler, H. C. Brown, D. H. Mitchell and E. N. Silvius, Dexmedetomidine: a novel sedative-analgesic agent, *Proc. (Bayl. Univ. Med. Cent.)*, 2001, **14**(1), 13–21.
18 A. Pertovaara, A. Haapalinna, J. Sirvio and R. Virtanen, Pharmacological properties, central nervous system effects, and potential therapeutic applications of atipamezole, a selective alpha2-adrenoceptor antagonist, *CNS Drug Rev.*, 2005, **11**(3), 273–288.
19 E. J. Beltran, C. M. Papadopoulos, S. Y. Tsai, G. L. Kartje and W. A. Wolf, Long-term motor improvement after stroke is

enhanced by short-term treatment with the alpha-2 antagonist, atipamezole, *Brain Res.*, 2010, **1346**, 174–182.

20 J. Sallinen, J. Rouru, J. Lehtimaki, P. Marjamäki, M. Haaparanta-Solin, E. Arponen, S. Helin, O. Solin, F. Tarazi and M. Shahid, ORM-12741: Receptor Pharmacology of a Novel Alpha2C-Adrenergic Receptor Subtype Selective Antagonist with Multi-therapeutic Potential, *Neuropsychopharmacology*, 2013, **38**, S558.

21 J. Rouru, K. Wesnes, J. Hänninen, M. Murphy, H. Riordan and J. Rinne, Safety and efficacy of ORM-12741 on cognitive and behavioral symptoms in patients with Alzheimer's disease: A randomized, double-blind, placebo-controlled, parallel group, multicenter, proof-of-concept 12 week study, *Neurology*, 2013, **80**(19), E201.

22 L. Ostopovici-Halip, R. Curpan, M. Mracec and C. G. Bologa, Structural determinants of the alpha2 adrenoceptor subtype selectivity, *J. Mol. Graphics Modell.*, 2011, **29**(8), 1030–1038.

23 D. J. J. Waugh, R. J. Gaivin, D. S. Damron, P. A. Murray and D. M. Perez, Binding, partial agonism, and potentiation of α-adrenergic receptor function by benzodiazepines: A potential site of allosteric modulation, *J. Pharmacol. Exp. Ther.*, 1999, **291**(3), 1164–1171.

24 D. E. Knutson, R. Roni, Y. Mian, J. M. Cook, D. C. Stafford and L. A. Arnold, Improved scale-up synthesis and purification of clinical asthma candidate MIDD0301, *Org. Process Res. Dev.*, 2020, **24**(8), 1467–1476.

25 M. D. Charles, P. Schultz and S. L. Buchwald, Efficient Pd-catalyzed amination of heteroaryl halides, *Org. Lett.*, 2005, **7**(18), 3965–3968.

26 H. G. Bonacorso, M. B. Rodrigues, B. A. Iglesias, C. H. da Silveira, S. C. Feitosa, W. C. Rosa, M. A. P. Martins, C. P. Frizzo and N. Zanatta, New 2-(aryl/heteroaryl)-6-(morpholin-4-yl/pyrrolidin-1-yl)-(4-trifluoromethyl)quinolines: synthesis Buchwald-Hartwig amination, photophysics, and biomolecular binding properties, *New J. Chem.*, 2018, **42**(12), 10024–10035.

27 **https://www.sigmaaldrich.com/US/en/services/software-and-digital-platforms/catalexis-catalyst-screening-platform**.

28 K. W. Anderson, R. E. Tundel, T. Ikawa, R. A. Altman and S. L. Buchwald, Monodentate phosphines provide highly active catalysts for Pd-catalyzed C-N bond-forming reactions of heteroaromatic halides/amines and (H)N-heterocycles, *Angew. Chem., Int. Ed.*, 2006, **45**(39), 6523–6527.

29 J. Besnard, G. F. Ruda, V. Setola, K. Abecassis, R. M. Rodriguiz, X. P. Huang, S. Norval, M. F. Sassano, A. I. Shin, L. A. Webster, F. R. Simeons, L. Stojanovski, A. Prat, N. G. Seidah, D. B. Constam, G. R. Bickerton, K. D. Read, W. C. Wetsel, I. H. Gilbert, B. L. Roth and A. L. Hopkins, Automated design of ligands to polypharmacological profiles, *Nature*, 2012, **492**(7428), 215–220.

30 W. K. Kroeze, M. F. Sassano, X. P. Huang, K. Lansu, J. D. McCorvy, P. M. Giguère, N. Sciaky and B. L. Roth, PRESTO-Tango as an open-source resource for interrogation of the druggable human GPCRome, *Nat. Struct. Mol. Biol.*, 2015, **22**(5), 362–369.

31 S. Uhlen, A. C. Porter and R. R. Neubig, The novel alpha-2 adrenergic radioligand [3H]-MK912 is alpha-2C selective among human alpha-2A, alpha-2B and alpha-2C adrenoceptors, *J. Pharmacol. Exp. Ther.*, 1994, **271**(3), 1558–1565.

32 L. Qu, Q. T. Zhou, D. Wu and S. W. Zhao, Crystal structures of the alpha2A adrenergic receptor in complex with an antagonist RSC, PDBj, 2019, DOI: **10.2210/pdb6kux/pdb**.

33 D. Yuan, Z. Liu, J. Kaindl, S. Maeda, J. Zhao, X. Sun, J. Xu, P. Gmeiner, H. W. Wang and B. K. Kobilka, Activation of the alpha(2B) adrenoceptor by the sedative sympatholytic dexmedetomidine, *Nat. Chem. Biol.*, 2020, **16**(5), 507–512.

34 X. Y. Chen, L. J. Wu, D. Wu and G. S. Zhong, Crystal structure of human alpha2C adrenergic G protein-coupled receptor, PDBj, 2019, DOI: **10.2210/pdb6KUW/pdb**.

35 P. P. Lakhlani, L. B. MacMillan, T. Z. Guo, B. A. McCool, D. M. Lovinger, M. Maze and L. E. Limbird, Substitution of a mutant alpha(2a)-adrenergic receptor via "hit and run" gene targeting reveals the role of this subtype in sedative, analgesic, and anesthetic-sparing responses in vivo, *Proc. Natl. Acad. Sci. U. S. A.*, 1997, **94**(18), 9950–9955.

36 N. T. Yücel, K. Ümmühan, Ü. D. Özkay and Ö. D. Can, 5-HT Serotonergic, α-Adrenergic and Opioidergic Receptors Mediate the Analgesic Efficacy of Vortioxetine in Mice, *Molecules*, 2021, **26**(11), 3242.

37 J. Lähdesmäki, J. Sallinen, E. MacDonald, J. Sirviö and M. Scheinin, α-adrenergic drug effects on brain monoamines, locomotion, and body temperature are largely abolished in mice lacking the α-adrenoceptor subtype, *Neuropharmacology*, 2003, **44**(7), 882–892.